 doi:10.20944/preprints202207.0277.v1

Article

Study on the Effect of Hydrothermal Carbonization Parameters on Fuel Properties of Chicken Manure Hydrochar

Małgorzata Hejna, Kacper Świechowski, Waheed A. Rasaq and Andrzej Białowiec *

Department of Applied Bioeconomy, Wrocław University of Environmental and Life Sciences, 37a Chełmońskiego Str., 51-630 Wrocław, Poland; malgorzata.hejna@upwr.edu.pl (M.H.); kacper.swiechowski@upwr.edu.pl (K.Ś.), waheed.rasaq@upwr.edu.pl (W.A.R)

* Correspondence: andrzej.bialowiec@upwr.edu.pl

Abstract: Economic development and population growth lead to increased production of chicken manure (CM), which is a problematic organic waste for its amount, environmental threats, and moisture content. There are different ways of CM, namely anaerobic digestion, composting, combustion, and direct land spreading. Hydrothermal carbonization (HTC) is another emerging way, however. In this study, the HTC of CM was performed to produce energy-rich material called hydrochar (HC). The effects of HTC temperature (180, 240, 300 °C) and process time (30, 90, 180 min) were summarized. Proximate and ultimate analysis, as well as heating values (HHV, LHV), have been performed both on raw CM and derived HC. Additionally, the process performance has been examined. The obtained results show that HTC is a feasible method for CM disposal and valorization. Although process time did not influence considerably fuel properties of CM, higher temperature led to significantly higher HHV, reaching 23,880.67±34.56 J×g^{-1} at 300 °C and 180 min with an improvement of ~8,329 J×g^{-1} compared with raw CM (15,551.67 J×g^{-1}). The process conducted at 240 °C in 30 min has been specified as the most favorable, due to the highest energy gain of HC and relatively low energy consumption.

Keywords: organic waste; waste to energy; waste to carbon; solid fuel; hydrochar; temperature; hydrothermal treatment

1. Introduction

1.1. Background

Modern poultry production and the increased associated waste, particularly excreta/manure, around the globe continue to pose a wide array of complex environmental challenges [1, 2]. For instance, given the increasing global number of chickens and laying hens, the produced waste inevitably becomes challenging to tackle [1]. Poultry manure is an example of organic waste, and it becomes a challenge to appropriately manage its bigger amounts emerging annually. Only Poland, which is a leader in poultry production in Europe, bred around 192.1 million birds in 2017, generating yearly approximately 4.5 million Mg of poultry manure [3, 4]. The most bred poultry is chicken, and its production is responsible for generating around 20,708 million Mg of manure worldwide each year [5]. Chicken manure is a problematic waste considering its amount, as well as high moisture content, which hampers transportation and management solutions. Waste generated in poultry farms, such as droppings and litter could pose human health risks [6]. In the wake of climate changes and energy shortages, there is an increasing need for new ways of providing clean and sustainable energy [7, 8]. In this sense, creating an alternative use of poultry manure for energy production purposes while mitigating its inherent effect on the environment is warranted, for instance, the application of thermochemical conversion processes such as pyrolysis, gasification, and direct burning of poultry manure to provide sustainable fuel [9].

 doi:10.20944/preprints202207.0277.v1

1.2. Chicken manure treatment

Ways of chicken waste disposal or management include: a) anaerobic digestion, for the management of chicken manure (CM), offers advantages including odor removal, carbon neutral biofuel, production of organic fertilizer in the form of liquid digestate by-product that contributes to tackling global warming and climate change; b) composting: as an alternative way of CM management to serve as organic fertilizer for crops, of which the content of pure nitrogen (N), potassium (K_2O) and phosphorus (P_2O_5) are about 1.63, 0.085, and 1.54%, respectively; c) combustion: as a process to offer an energy recovery from CM, combustion is often used to power incineration facilities; d) direct land spreading: the application of CM in the form of direct spread on land as a fertilizer for crops [10, 11].

Despite those applications, hydrothermal carbonization (HTC) is considered a suitable way of CM management, for it is environmentally friendly in the context of emission compared to other processes, especially composting process, with its ammonia emissions to the atmosphere [9, 12], feasible process and the low-cost benefit over other treatment, and a viable way to valorize the digestate in an energy-efficient manner and at the same time maximize the synergy in terms of recovery of water, nutrients, followed by more efficient use of the remaining carbon [13]. Another benefit of HTC is that there is no need for manure drying, which is directly related to the emission of odors. The hydrothermal conversion process of recycling organic waste or biomass in general usually begins at the temperature range of 160 and 300 °C [8, 9, 14]. Largely, this depends on the type of hydrothermal treatment and purpose of any given (hydrothermal conversion process-based) project. Generally, the hydrothermal treatment process comprises different categories, namely: hydrothermal carbonization or liquefaction (HTC/L) [8, 14, 15]. These types could also be classified based on operational conditions.

1.3. Hydrothermal carbonization

In this work, the application of HTC is considered due to its feasible process and the low-cost benefit over pyrolysis type treatment. Hydrothermal treatment is gaining popularity as one of the methods to effectively manage organic waste characterized by high moisture content (MC), for the process does not require pre-drying, resulting in being more attractive [16]. The process of HTC strongly imitates the natural processes of coal shaping [17]. It occurs in conditions of subcritical water at temperatures usually ranging from 180 to 350 °C and under autogenous pressure generated during the process of carbonization with a residence time of 30 min to several hours [18–21]. The mechanisms of the HTC process vary depending on the used material type, however, two main reactions occurring are dehydration and decarboxylation, leading to water and CO_2 removal from the biomass material [9, 14–16]. As a thermal valorization process, it operates effectively on biomass with high MC (70–90%) compared to conventional thermal technologies like dry torrefaction and pyrolysis, which require pre-drying process that entails additional energy usage and causes problems with odor emission [22]. The energy requirements that are engaged within the production of hydrochar (HC), which is the main product of the HTC process, are believed to be much less compared to those required for thermal conversion treatment with higher operating conditions. Whilst pyrolysis temperature at 600 °C or higher increased the production of gases and liquid fractions at the expense of solid fractions and the ultimate loss of the carbonized solid fuel's (CSF's) calorific values [20, 21], thermochemical processes that underpin HTC are considered among potentially green methods able to deconstruct biomass. Thus, the HTC process presents merits given its enhanced process performance, and at the same time, environmental-friendly and technologically innovative approach [22]. In the HTC operating process, the feedstock particle size [23], would impact the overall energy and production yield. Variations in pressure and temperature facilitate the solvent's interaction between intermolecular forces [22], there are liquefaction aspects, where the involved biomass undergoes reactions such as depolymerization, decomposition, and recombination, which are dependent on the

 doi:10.20944/preprints202207.0277.v1

reactive nature. Previous reviews about thermal conversion [8] have emphasized the fundamental processes/mechanisms involving HTC, where various research needs, and characterization of products have led to the identification of its deemed importance in industrial applications.

The increases in globally generated chicken manure call for improved thermal conversion/pre-treatment-oriented solutions. The use of manure as an energy source via HTC process and slow pyrolysis for the HC production and biochar respectively appears promising, given the evidence of its impact of the reaction temperature on the HC yields and quality of chicken manure [24]. HC would have a higher heating value, higher energy yield, and lower ash content with respect to the same feedstock compared to biochar and the HC from chicken manure of 64.4% at 210 °C [25]. In addition, the treatment temperature and residence time have an influence on the composition of HC and the yield using poultry manure. The temperature had a significant effect leading to the enhancement of HHV by up to 25.17% at 250 °C, while resident time had less impact, and ash recovery, in the HC, was between 74.67 and 36.59%, respectively [26]. Key properties considered of HC for energy purposes include mass yield, energy densification ratio, and energy yield.

1.4. Study aim

Thermal transformation of waste groups still needs further studies, in fact, there appears to be a paucity of research on HTC treatment of poultry manure, specifically the impact on hydrochar's chemical and physical properties. Such findings can also be used to process kinetic determination and to model the energy balance of HTC of the organic waste [27, 28]. On this premise, the current investigation critically analyzed the HTC process of chicken manure and its energetic potential using a lab-scale pressure reactor. In particular, the specific objectives included: a) determination of the operating conditions (temperature, duration, and pressure) effects on the HTC performance and b) characterization of the fuel properties of HC produced from chicken manure.

2. Materials and Methods

2.1. Material (Feedstock)

Chicken manure was obtained from a farm located at the Agricultural Experiment Station Swojec that belongs to the Wroclaw University of Environmental and Life Sciences (Wroclaw Poland). The fresh chicken manure (CM), which was up to 1 day old, was collected directly from under the cages using a metal spade and placed into two plastic buckets with a capacity of 10 liters. The CM was then mixed using a drill (Bosch, model Professional GSB 16 RE, Gerlingen, Germany) with a mortar stirrer to obtain homogeneity and separated into samples of 250 grams. Such prepared samples were then placed in the freezer (Electrolux, model EC5231A0W, Stockholm, Sweden) at the temperature of –27 °C until further use.

2.2. Methods

2.2.1. HTC process – hydrochar production

The HTC process was performed using a high-temperature high-pressure reactor (HPHT) (Büchi AG, Uster, Switzerland).

The sample of 220 grams of CM, theretofore thawed, was placed in the feedstock vessel, which was then placed in the heating jacket, closed, and sealed. The speed of the stirrer was set to 120 rpm and the desired temperature inside the vessel was set. The HTC processes were carried out at three different temperatures of 180, 240 and 300 °C. After reaching the temperature of 5 °C lower than the set value, the process continued for 0,5, 1,5 and 3 hours (it was because of the PID temperature controller, which needs a lot of time to heat up the reactor by the last 5 °C). Each temperature was combined with each retention time three times to ensure repeatability. After the specified time has elapsed, the reactor was set to cool down. During the process, the pressure was generated autogenously. Additionally, during the process, the energy consumption was recorded using an

Preprints (www.preprints.org) | NOT PEER-REVIEWED | Posted: 19 July 2022 doi:10.20944/preprints202207.0277.v1

energy meter (Starmeter Instruments Co. Ltd., SK-410, Shenzhen, China). After reaching the temperature of 45 °C, the reactor was turned off, the valve was opened to release pressure and the sample was removed from the vessel using a plastic spoon. The sample was then weighed using a laboratory scale (Radwag, MA 50.R, Morawica, Poland) and the solid part was separated from the liquid using a vacuum filtration (Rocker, ROCKER 300, Kaohsiung, Taiwan). The liquid part was placed into a plastic container and placed in the freezer (Electrolux, model EC5231A0W, Stockholm, Sweden) at a temperature of –27 °C. The solid part was weighed and placed into a laboratory dryer (WAMED, KBC-65W, Warsaw, Poland) for 24 hours at 105 °C. After that time, the obtained HC sample was ground using an electric grinder (Royal Catering, RCMZ-800, Wuppertal, Germany) and sieved through a 0.025 mm mesh sieve to homogenize the material. Fractions below 0.025 mm were stored in plastic bags until further analyses.

2.2.2. Hydrochar fuel properties analyses

Raw and processed samples were tested in three replicates to ensure repeatability. The moisture content (MC) was determined in accordance with Świechowski et al. (2019) [30], using a laboratory dryer (WAMED, KBC-65W, Warsaw, Poland). The volatile matter content (VM) was measured via the thermogravimetric method by means of a tubular furnace (Czylok, RST 40 × 200/100, Jastrzębie-Zdrój, Poland), in accordance with Torquato et al. (2017) [31]. The ash content (AC) was determined by incinerating the sample in a muffle furnace (Snol 8.1/1100, Utena, Lithuania) in accordance with PN-Z-15008-04:1993 standard. Fixed carbon (FC) was determined by the difference between VM and AC. Samples were also tested for the content of volatile solids (VS), according to PN-EN 15935:2022-01 standard [32], by means of the muffle furnace (Snol 8.1/1100, Utena, Lithuania). The high heating value (HHV) was determined using a calorimeter (IKA, C200, Staufen, Germany), in accordance with PN EN ISO 18125:2017-07 standard [33].

Fuel ratio was calculated using Equation (1) [34].

$$FR = \frac{FC}{VM} \quad (1)$$

where:
FR—fuel ratio, -.
FC—fixed carbon, %
VM—volatile matter, %.

The low heating value (LHV) was calculated based on Equation (2) [3].

$$LHV = HHV - 2{,}441.8 \times \left(9 \times \frac{H}{100}\right) - 24.41 \times \left(\frac{MC}{100}\right) \times \left(100 - \frac{MC}{100}\right) \quad (2)$$

where:
LHV—low heating value (as dry base), J×g^{-1};
HHV—high heating value (as dry base), J×g^{-1};
H—hydrogen content, %;
MC—moisture content, %;

The content of carbon, hydrogen, nitrogen, and sulfur elements was determined using an elemental analyzer (Perkin Elmer, 2400 Series, Waltham, USA) according to PN-EN ISO 16948:2015-07 standard [32]. The oxygen content was calculated based on Equation (3) [10].

$$O = 100\% - C - H - N - S - AC \quad (3)$$

where:
O—oxygen content, %;
C—carbon content, %;
N—nitrogen content, %;
S—sulfur content, %;
AC—ash content, %.

Preprints (www.preprints.org) | NOT PEER-REVIEWED | Posted: 19 July 2022 doi:10.20944/preprints202207.0277.v1

Additionally, the H/C and O/C ratios were calculated based on Equations (4) and (5) [37].

$$H/C = \frac{\frac{H}{1}}{\frac{C}{12}} \quad (4)$$

$$O/C = \frac{\frac{O}{16}}{\frac{C}{12}} \quad (5)$$

where:
H/C—molar ratio of H to C, -;
O/C—molar ratio of O to C, -;
1—molar mass of H, u;
12—molar mass of C, u;
16—molar mass of O, u.

2.2.3. Hydrothermal carbonization performance

The mass yield (MY) was calculated based on Equation (6). The energy densification ratio (EDr) was determined using Equation (7). Energy yield (EY) was calculated based on Equation (8) [30].

$$MY = \frac{m_h}{m_r} \times 100 \quad (6)$$

$$EDr = \frac{HHV_h}{HHV_r} \times 100 \quad (7)$$

$$EY = MY \times EDr \quad (8)$$

where:
MY—mass yield, %;
m_h—mass of dry hydrochar after HTC process, g;
m_r—mass of dry raw material before HTC process, g;
ED_r— energy densification ratio, %;
HHV_h—high heating value of hydrochar after HTC process, J×g^{-1};
HHV_r—high heating value of raw material before HTC process, J×g^{-1};
EY—energy yield, %.

Additionally, to establish the most advantageous process conditions, the energy gain (EG) has been calculated using Equation (9) [38].

$$EG = \frac{(HHV_h - HHV_r)/HHV_r}{(m_r - m_h)/m_r} \times 100 \quad (9)$$

where:
EG—energy gain, %.

2.2.4. Statistical analysis

The two-way analysis of variance (ANOVA) with post-hoc Tukey tests was performed at the level of α = 0.05 to find statistically significant differences. Statistica 13.0 software (TIBCO Software Inc., Palo Alto, CA, USA) was used for this purpose. Results obtained during statistical analysis are presented in Appendix A (Tables A1-A17).

Preprints (www.preprints.org) | NOT PEER-REVIEWED | Posted: 19 July 2022 doi:10.20944/preprints202207.0277.v1

3. Results and discussion

3.1. Properties of raw chicken manure

The chicken manure used in this experiment contains 70.58±3.65% of moisture, which proves that it is a suitable material for the HTC process. Feedstock with MC ranging from 75% to 90% appears to be ideal for this process [38]. The results of the proximate, ultimate, and HHV analyses performed on the raw material used in this study are shown in Table 1. The data was compiled with the results of studies performed by other researchers [3, 38, 39]. The VM content in CM appears to be higher in comparison to other results. As for the AC content, it is an intermediate value compared to others' results, and Hussein et al. (2017) obtained a very similar result of 21.65% of AC [40]. The FC value is lower than FC in other CM presented in the literature, which is not a preferable result, as a high FC value indicates that the fuel may successfully replace conventional fossil fuels [41]. However, the FC content in poultry litter in general ranges from 6% to 23% [3]. Both C and H contents are similar to the ones found in literature, however, N and S contents appear to be higher. The high amount of N may be caused by the high amount of protein and uric acid [42]. The high content of S and N is inadvisable in fuel as these elements are responsible for the emissions of SOx and NOx emissions which consequently pollute the environment [43]. The HHV of the studied CM was 15,551.67±53.82 J×g^{-1} and was higher than the typical CM (Table 1). The same can be observed for LHV, which is 4,232.89±367.20 J×g^{-1} and is higher than LHV of chicken manure HC obtained by Tańczuk et al. (2019) by 1,031.89 J×g^{-1} [3].

Table 1. Results of proximate, ultimate, and heating value analysis for raw chicken manure.

Properties	**CM (this study)**	**Other studies**		
		CM1 [39]	**CM2 [3]**	**CM3 [38]**
Proximate Analysis (%)*				
VM	70.35±0.23	69.23	67.50	48.79
AC	21.12±0.47	11.64	15.60	34.70
FC	8.53±0.38	19.13	16.90	16.51
VS	78.88±0.47	-	-	-
Ultimate Analysis (%)*				
C	37.46±1.19	31.54	39.67	30.04
H	5.22±0.12	4.52	4.72	4.32
N	8.28±0.23	3.34	5.49	3.22
S	1.92+0.09	0.56	0.40	0.35
O	26.00+2.31	60.04	34.12	29.66
HHV (J×g^{-1})*	15,551.67±52.82	12,980.00	13,780.00	11,950.00
LHV (J×g^{-1})*	4,232.89±367.20	-	3,201.00	-

*as dry base

3.2. Fuel properties of hydrochar

Both temperature and retention time had an influence on hydrochars' properties, as well as on generated pressure (Table 2), however, the temperature's effect was more considerable.

Preprints (www.preprints.org) | NOT PEER-REVIEWED | Posted: 19 July 2022 doi:10.20944/preprints202207.0277.v1

Table 2. Proximate analysis and reached pressure of derived hydrochars.

Temperature (°C)	Time (min)	Pressure (bar)	VM (%)*	FC (%)*	FR (-)*	VS(%)*	AC (%)*
	30	6	67.90±0.45	10.36±0.79	0.15±0.01	78.26±0.93	21.74±1.07
180	90	10	67.48±0.53	10.46±0.26	0.16±0.01	77.94±0.65	22.06±0.72
	180	19	61.85±0.80	13.56±0.86	0.22±0.02	74.85±1.50	24.59±0.43
	30	44	57.45±1.19	14.30±1.11	0.25±0.02	61.77±2.32	28.25±0.91
240	90	48	55.17±0.95	13.56±0.53	0.25±0.01	65.37±6.10	31.26±0.49
	180	46	40.14±0.86	27.89±0.89	0.70±0.04	60.00±8.35	31.97±0.24
	30	103	44.22±0.51	25.68±0.53	0.58±0.02	59.99±4.99	30.10±0.02
300	90	98	41.91±1.39	27.20±1.05	0.65±0.05	57.92±4.89	30.89±0.82
	180	101	37.48±1.25	30.33±1.28	0.81±0.06	58.13±6.66	32.20±0.21

*as dry base

The FC content has increased, while the VM and VS content has reduced. The highest increase in FC value was observed at 240 °C with an increase of 255.59% relative to raw CM. The highest FC content was obtained in HC derived at 300 °C at 180 min (30.33±1.28%) and the result was 192.65% higher than FC content in HC obtained at the lowest process parameters. The observed differences in FC content for parameters were significant ($p < 0.05$), and the same was observed for VM content (Table A1, Table A2). The lowest VM content was present in the HC derived in the highest parameters (300 °C, 180 min) with a value of 37.48±1.25%. The increase of FC content is caused by high temperature, which leads to the devolatilization of organic matter, and therefore a higher amount of solid carbon remains concerning the residual volatile matter [44]. The VS content decreased from 78.88±0.47% for raw CM to 57.92±4.89% for the HC obtained at 300 °C in 90 min. Low VM content is a desirable result, as it generates a higher amount of tar, which then leads to problems with combustion or gasification systems [45]. In comparison to HC obtained from different biomass feedstock, the VM content in this study was relatively low. For instance, HC derived from coconut fiber at temperatures from 220 to 375 °C, was ranging from 69.8% for the lowest temperature to 42.6% for the highest temperature. As shown by Feiyue et al. (2022), HC derived from CM at temperatures ranging from 200 to 350 °C in 120 min, was characterized by FC with the highest share of 15.74% for the temperature of 300 °C [46]. Moreover, the FC and VM content in lignite stands for 49.0% and 42.1%, respectively [47, 48]. This suggests that HC derived from CM has beneficial fuel properties.

The highest FR was 0.81±0.06 for HC derived at 300 °C in 180 min. It was observed that the fuel ratio increased with temperature and time increase (Table 2). Statistically significant differences among process parameters have been noted ($p < 0.05$) (Table A3). As the FR of all obtained samples of HC was < 2.5 (Table 2), it can be concluded that all produced hydrochars have an adequate combustion performance for pulverized fuel burning [47].

The AC content in fuel plays a vital role in the energy sector, as high AC may cause damage in furnaces, which is the effect of high alkali metals content, and it also increases costs of waste disposal after the combustion process [47]. The AC has increased from 21.12±0.47% in raw CM to 32.20±0.21% in HC derived at 300 °C at 180 min. This increase has also noted been by other researchers, for instance, the AC of corn stalk increased from 4.80% for raw material to 6.12% and 12.13% for 200 °C and 250 °C, respectively [49]. The increase of AC is caused by decreased mass yield and exceeding loss in organic material over inorganic material [49]. Also, the statement posed by Burra et al. (2016) [50] that CM is rich in ash when compared to other biomass sources, has been confirmed. For instance, the AC present in HC obtained from dead leaves at temperatures from 200 °C to 250 °C ranged from 13.64% to 21.04% [51], which is also lower than observed in this study. For watermelon peel, the AC ranged from 4.19% to 6.24% in HC derived at temperatures from 190 to 260 °C [52].

Preprints (www.preprints.org) | NOT PEER-REVIEWED | Posted: 19 July 2022 doi:10.20944/preprints202207.0277.v1

The results of elemental analysis are presented in Table 3. As expected, the C content increased with temperature, while the O content decreased.

Table 3. Elemental analysis of derived hydrochars.

Temperature (°C)	Time (min)	C (%)*	H (%)*	N (%)*	S (%)*	O (%)*
180	30	40.48±0.23	5.20±0.07	7.83±0.50	1.79±0.06	22.97±0.59
	90	42.52±0.51	5.14±0.02	7.60±0.36	1.93±0.04	20.74±0.75
	180	43.41±1.45	4.89±0.06	7.38±0.41	1.83±0.12	17.90±1.72
240	30	46.09±0.58	4.78±0.11	5.59±0.30	1.98±0.05	13.31±1.23
	90	47.34±0.22	4.60±0.11	5.40±0.19	1.97±0.03	9.43±1.06
	180	48.19±0.69	4.51±0.04	5.25±0.05	1.89±0.08	8.12±0.74
300	30	50.07±0.06	4.40±0.03	5.01±0.03	1.92±0.06	8.48±0.62
	90	51.46±1.51	4.38±0.04	4.91±0.04	1.88±0.16	6.47±1.25
	180	52.23±0.57	4.31±0.03	4.85±0.03	1.87±0.09	4.65±1.04

*as dry base

The highest C content was in HC derived at 300 °C in 180 min (52.23±0.57%). There were statistically significant differences when compared to other process parameters. The loss in O content (down to 4.65±1.04%) is favorable, as together with high C content it leads to an energy density increase [53]. There were no considerable changes in S content with both time and temperature, with an average share of 1.90%. Generally, the amount of S should decrease with the temperature increase [52, 54], however, according to Liu et al. (2013) and Devi & Karoha (2015), the S amount was remaining stable [34, 48]. HCs derived from different materials, e.g. HCs derived from beet pulp and dry leaves do not contain any S, regardless of temperature changes. The N content was decreasing with both time and temperature, with a decrease of 58.53% in comparison to raw material, reaching 4.85±0.03% N in CM derived at the highest process parameters. However, the N content was also higher than in HCs described above [51, 54]. According to Ashworth et al. (2020), poultry manure contains essential plant nutrients, including N and S. Moreover, CM contains more N and S than other poultry manure, eg. turkey manure [55, 56]. Although these elements are not favorable in relation to combustion (as mentioned in paragraph 3.1.), it suggests that further investigation would provide additional meaningful insight into fertilizer properties of HC derived from CM, but also fertilizer properties of the liquid fraction which is a by-product of the HTC process.

The Van Krevelen diagram (Figure 1) was used to present the fuel properties of derived HC by comparison of H/C and O/C ratios. Both values decrease as the process temperature increases. On the diagram, the positions of the HCs derived at lower parameters

Preprints (www.preprints.org) | NOT PEER-REVIEWED | Posted: 19 July 2022 doi:10.20944/preprints202207.0277.v1

(as for time and temperature) were closer to the range of biomass and peat, while the HCs obtained at higher parameters are more similar to lignite and coal.

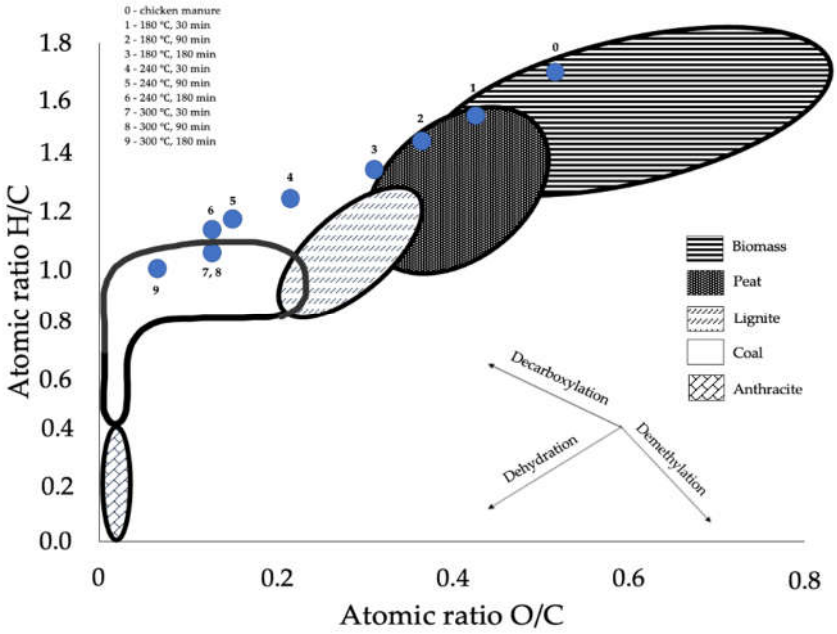

Figure 1. Van Krevelen's diagram of raw and HTC treated chicken manure.

An HHV refers to the highest possible energy that is released through the full oxidation process of one fuel unit [57]. As can be seen in Figure 2, the HHV of HC increased with the increase of both temperature and time.

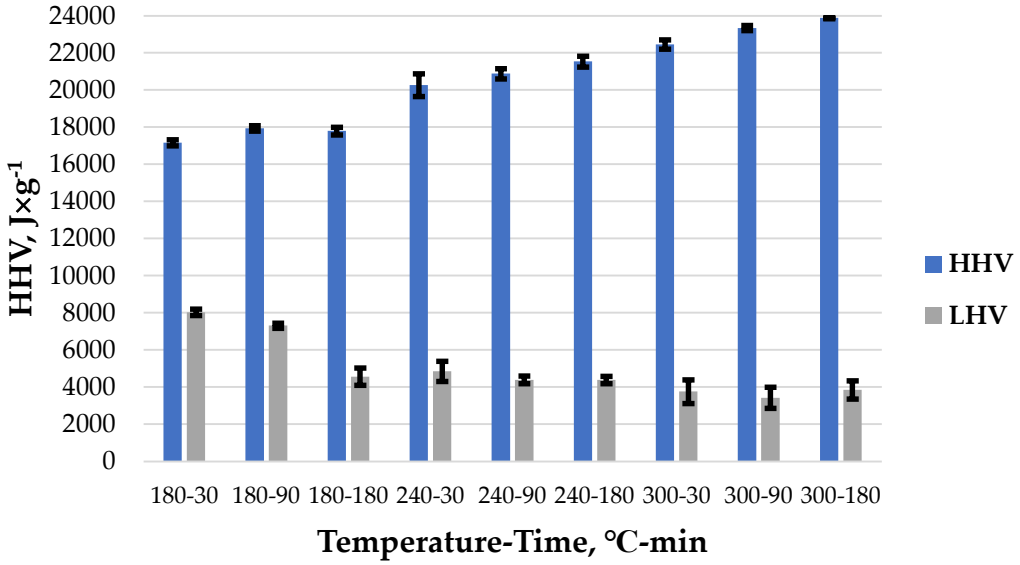

Figure 2. High and low heating value for obtained hydrochar.

The HC derived at 300 °C in 180 min was characterized by the highest HHV (23,880.67±34.56 J×g^{-1}). The difference between this HC and raw CM is ~8,329 J×g^{-1}. The difference in HHV was statistically significantly different ($p < 0.05$) (Table A4). HTC of CM leads to the production of fuel with relatively high HHV, as lignite is characterized by HHV of ~30 MJ×kg^{-1} [47]. What is more, this value is similar to HCs obtained from some other types of biomass. For instance, grape pomace converted at 300 °C in 30 min reached HHV of 25.29 MJ×kg^{-1}, and corn stover carbonized at 300 °C in 77 min reached

Preprints (www.preprints.org) | NOT PEER-REVIEWED | Posted: 19 July 2022 doi:10.20944/preprints202207.0277.v1

HHV of 27,470.00 J×g^{-1}. The obtained result is also higher when compared to wood materials. For instance, spruce wood and beech wood were characterized by 20.4 and 19.3 MJ×kg^{-1}, respectively [58]. LHV value, which allows for determining the actual energy potential of biomass [59], was decreasing with higher parameters of the HTC process (Figure 2), which is related to the amount of solid phase obtained during the process. The LHV decreased from 8,030.10±494.63 J×g^{-1} (180 °C-30 min) to 3,410.45±570.11 J×g^{-1} for HC obtained at 300 °C in 90 min. What is more, the LHV value was higher for HC obtained at 180 and 240 °C than raw chicken manure (4,232.89±367.20 J×g^{-1}), whereas the LHV of HC obtained at 300 °C was lower.

3.3. Hydrochar and HTC energy yields

Figure 3 shows an example of temperatures and pressure patterns during the HTC process. The average heating rate was ~4.9, ~4.0, and ~3.8 °C×min^{-1} for 180, 240, and 300 °C, respectively.

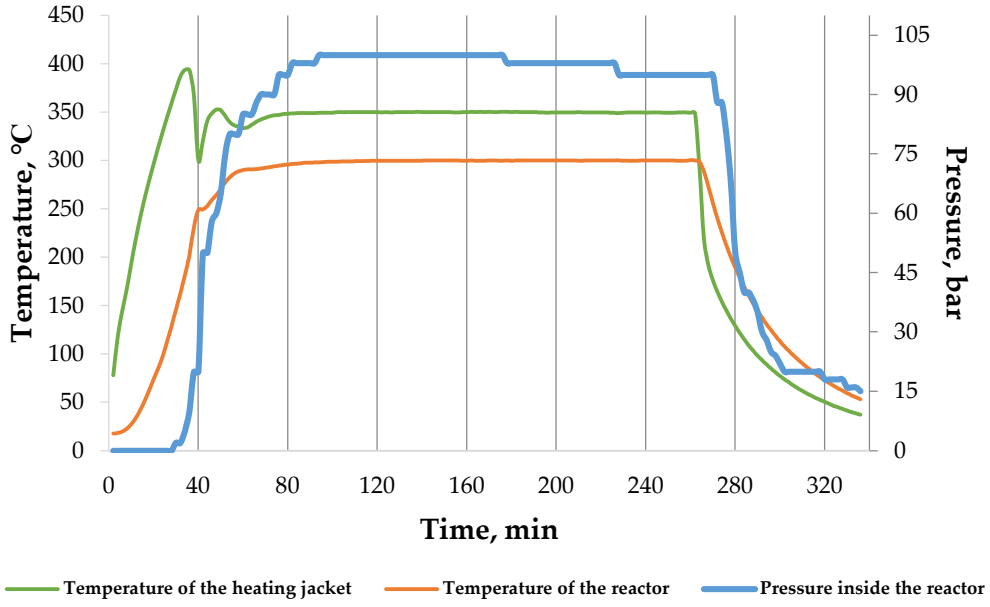

Figure 3. An example of temperature and pressure patterns during the process at 300 °C in 180 min.

Graphs presenting temperature and pressure patterns during the HTC process with different parameters are available in appendix B (Figures B1–B8).

The increase in the pressure depended on the set temperature point and the amount of produced gas. While the amount of produced gas resulted from the decomposition of the processed material. In the performed study, the retention time did not lead to considerable HC yield change, which can be seen in Figure 4.

Preprints (www.preprints.org) | NOT PEER-REVIEWED | Posted: 19 July 2022 doi:10.20944/preprints202207.0277.v1

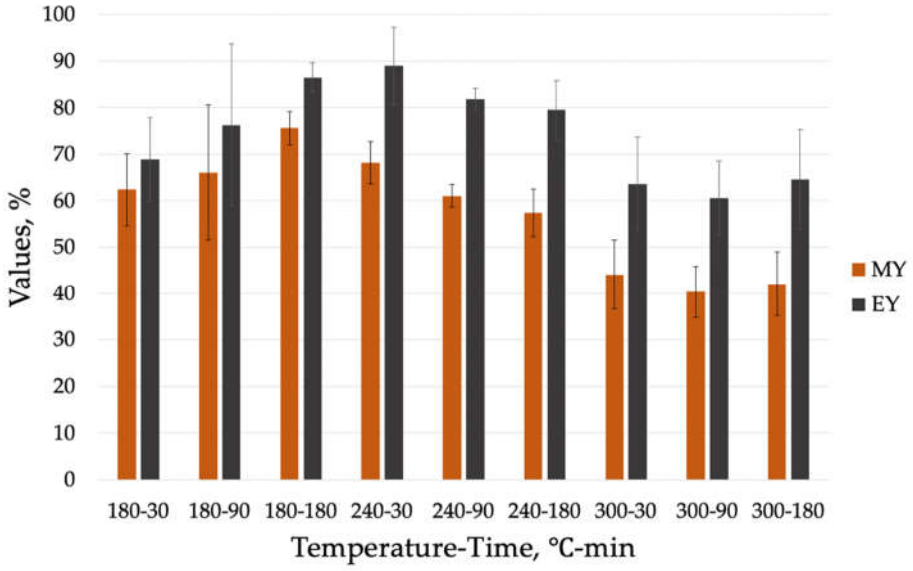

Figure 4. Hydrochar mass and energy yield in temperature and time.

The MY has decreased with time by 10.75 and 2.03 percent points at 240 and 300 °C, respectively. However, in the case of the processes running at 180 °C, the MY has increased by 13.21 percent points with time. In the literature, both cases of increase and decrease can be found [54, 60, 61]. The temperature inside the reactor had a more distinctive effect on the MY, leading to increased mass losses. The highest MY was observed for HC derived at 180 °C in 180 min (72.25±3.59%), while the MY was the lowest at 300 °C, generating in 90 min 40.37±5.53% of the solid phase (HC). The observed decrease in MY may be induced by the decarboxylation process and forming organic soluble in water. As poultry manure is rich in cellulose, with an average of 24.13%, it also leads to decomposition and depolymerization of this component, contributing to enhanced liquid and gaseous product formation [62, 63]. Similar trends have been reported by other researchers [47, 64]. The HC yield derived during performed HTC process is higher than the HC yield acquired from the HTC process performed by other researchers on different kinds of feedstock. For instance, HC obtained from swine manure at temperatures of 200 °C and 300 °C were 55.52% and 25.64%, respectively [46]. Wheat straw subjected to HTC process at 250 °C in 120 min reached 35.93% of MY. This lower yield might be caused by the composition of compared types of biomasses, e.g. wheat straw contains more cellulose than CM, reaching from 28% to 39% [65].

Energy yield is an important parameter, as it defines the amount of energy left in HC [47]. As presented in Figure 4, EY increased with time at 180 °C by 25.54%, and slightly at 300 °C by 1.62%. However, it decreased at 240 °C by 10.65%. Moreover, the HC obtained at 300 °C is characterized by the lowest EY, reaching 63.59±10.13%, 60.57±8.01% and 64.62±10.71% in 30, 90, and 180 min, respectively. The highest EY was from HC derived at 240 °C in 30 min (88.99±8.29%) (Figure 4). A decrease in EY with increasing temperature was also noted for HC obtained from poultry litter, but also for biochar obtained from the same material [45]. The decreasing trend of EY for HC with increasing temperature and time is common because of material decomposition and its conversion into liquid and gas products as well [64].

The energy densification ratio shows the increase in the energy content of HC concerning the raw substrate. The EDr was generally increasing with time and temperature ($p < 0.05$) (Table A5) (Figure 5).

Preprints (www.preprints.org) | NOT PEER-REVIEWED | Posted: 19 July 2022 doi:10.20944/preprints202207.0277.v1

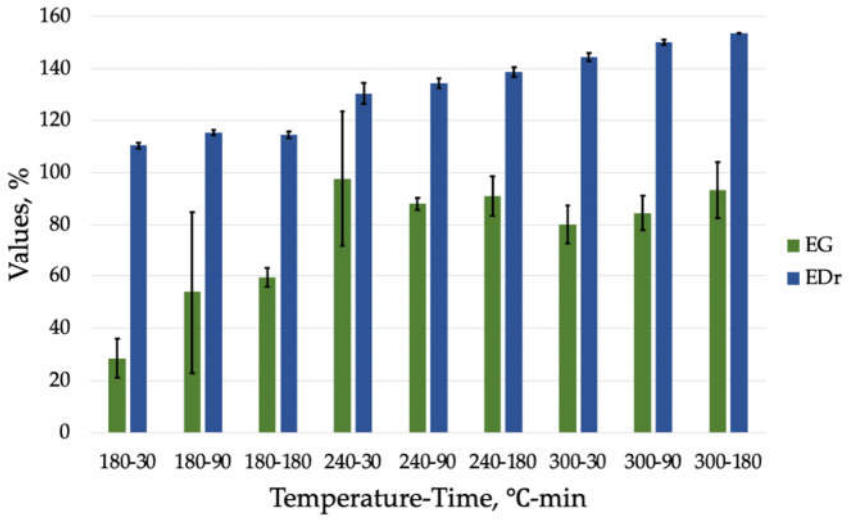

Figure 5. Hydrochar energy densification ratio and energy gain in temperature and time.

The highest value of EDr was obtained in HC produced at 300 °C in 180 min (153.56±0.22). Generally, the EDr tends to increase with higher temperatures, which was proved for wheat straw, corn cob, sunflower stalk, and dry leaves [49, 51]. Energy gain, which can determine the most favorable HTC conditions, shows the best compromise for mass and energy content in the derived HC. As shown in Figure 6, EG tends to increase with temperature and time increase. This correlation was also observed for the HTC process of eucalyptus-tree residues [37]. However, the highest EG was observed for HC obtained at 240 °C in 30 min, reaching 97.6±25.78%. A statistically significant difference was observed between this HC and products obtained at 180 °C in 30 and 90 min ($p < 0.05$) (Table A6). This leads to a conclusion, that HC derived at 240 °C in 30 min is more economically profitable, as it allows to generate more energy with a slightly higher temperature and shorter time. What is more, as presented in Figure 6, energy usage (Eu) tends to increase with both temperature and retention time, reaching 418,270±97,904 kJ×g^{-1} for HC obtained at 300 °C in 180 min, as for dry basis of obtained HC. The result for 240-30 was 124,336±8,286 kJ×g^{-1}, which is 1.56 times higher than for HC obtained in the lowest parameters and 3.36 times lower than HC obtained in the highest parameters of HTC.

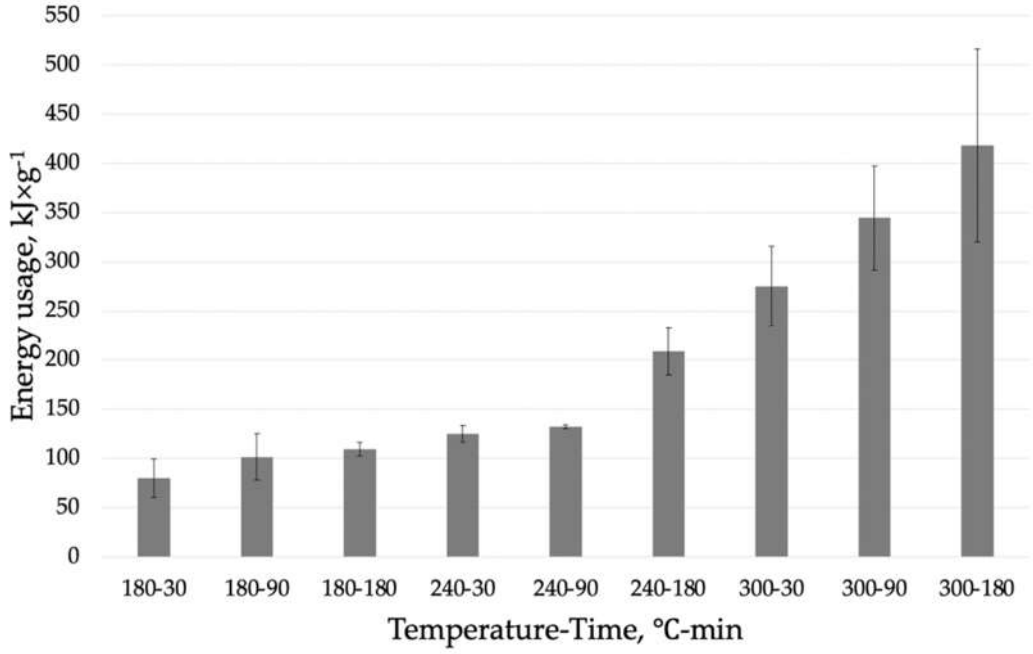

Figure 6. Energy usage of the HTC process in relation to the mass of dry hydrochar obtained after the process.

Preprints (www.preprints.org) | NOT PEER-REVIEWED | Posted: 19 July 2022 doi:10.20944/preprints202207.0277.v1

Additionally, energy usage in relation to one unit of energy available in one unit of obtained HC (Eg) has been calculated (Figure 7).

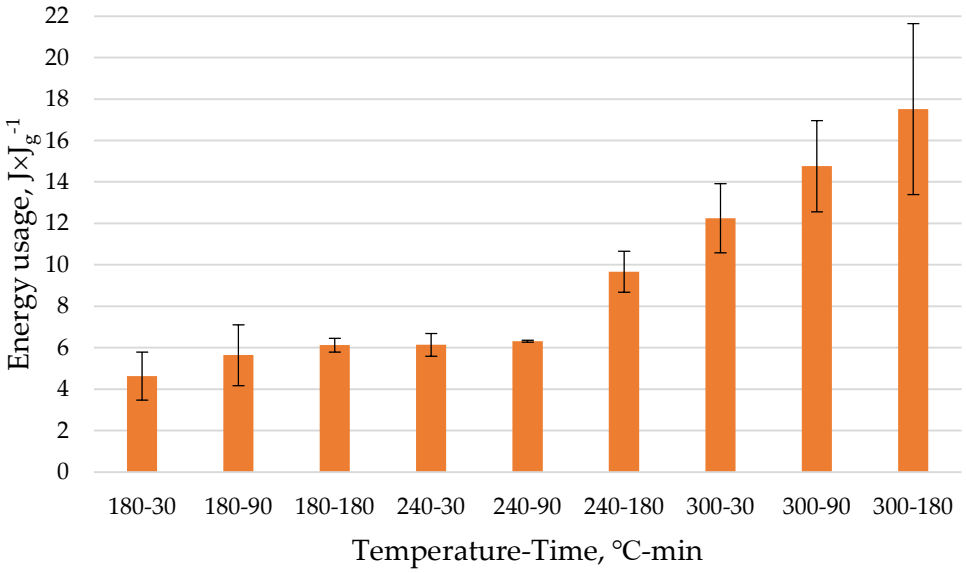

Figure 7. Energy usage in relation to one unit of energy available in one unit of obtained dry HC.

The highest result was obtained for HC derived in the highest process parameters (300 °C, 180 min) (17.52±4.12 J×J_g^{-1}). Moreover, the analysis of variance showed that there are no statistically significant differences ($p < 0.05$) (Table A7) between the amount of energy utilized for hydrochars produced at 180-30 and 240-90. There was also no significant difference between energy usage in relation to one unit of energy available in one unit of obtained HC for HC derived at 240 °C in 30 min and HC with the lowest energy usage (180 °C, 30 min; 4.64±1.64 J×J_g^{-1}). This confirms that the most favorable conditions for the poultry manure HTC process are 240 °C and 30 min since these parameters provide the best compromise between the amount of energy left in HC (Figure 5) and energy usage for its production (Figure 6).

5. Conclusions

Hydrothermal carbonization was proposed as a way of chicken manure disposal with rich-energy material production at the same time. Both temperature and time of the process had an influence on hydrochar production and its properties, however, the impact of increasing temperature was more significant than of increasing process duration.

Both proximate and ultimate analysis allowed to draw the conclusion, that hydrochar derived at the highest parameters (that is: 300 °C, 180 min) has the best fuel parameters. The FC, AC and VM contents were 30.33±1.28, 32.20±0.21 and 37.48±1.25%, respectively. The H/C and O/C ratios were 0.99±0.02 and 0.07±0.01, respectively. The HHV reached 23,880.67±34.56 J×g^{-1}, and LHV for this HC was 3,850.94±494.63. These results indicate that higher temperatures lead to more completed decomposition reactions and energy densification. However, the energy consumption for this process was high (418.27±97.91 kJ×g^{-1} as for dry HC obtained after the process), indicating that these parameters may not be efficient.

Considering the EG, the HC derived at 240 °C in 30 min has the best result. Moreover, the energy consumption for this process was relatively low (124.34±8.29 kJ×g^{-1}). With its still feasible fuel properties and HHV of 20267.00±617.83 kJ×g^{-1}, it has been concluded that these parameters of HTC of CM are the most beneficial.

The high N and S content in derived HC incline further investigation on CM HC fertilizer properties, but also to investigate the possible properties of liquid fractions obtained during the HTC process as a by-product.

 doi:10.20944/preprints202207.0277.v1

Supplementary Materials: Figure S1: title; Table S1: title; Video S1: title.

Author Contributions: Conceptualization, M.H., K.Ś. and A.B.; methodology, M.H. and K.Ś.; software, M.H.; validation, M.H. and K.Ś.; formal analysis, M.H.; investigation, M.H. and W.A.R.; resources, M.H. and K.Ś.; data curation, M.H. and K.Ś.; writing—original draft preparation, M.H. and W.A.R.; writing—review and editing, M.H., K.Ś., A.B. and W.A.R.; visualization, M.H.; supervision, A.B.; project administration, M.H.; funding acquisition, A.B. All authors have read and agreed to the published version of the manuscript.

Funding: This research was funded by WROCŁAW UNIVERSITY OF ENVIRONMENTAL AND LIFE SCIENCES, grant number N010/005/21.

Data Availability Statement: All data generated and used in the study is available in the article and Supplementary Materials.

Conflicts of Interest: The authors declare no conflict of interest.

Preprints (www.preprints.org) | NOT PEER-REVIEWED | Posted: 19 July 2022 doi:10.20944/preprints202207.0277.v1

Appendix A

Appendix A contains a statistical analysis of the results presented in the article. Bold font signifies a statistically significant difference ($p < 0.05$) between particular process parameters, e.g. 180-30 refers to 180 °C and 30 min.

Table A1. Two-way analysis of variance (ANOVA) with post-hoc Tukey test for FC content, a bold font signifies a statistically significant difference ($p < 0.05$).

Temp-Time	180-30	180-90	180-180	240-30	240-90	240-180	300-30	300-90	300-180
180-30		1.000000	**0.002551**	**0.000402**	**0.002540**	**0.000179**	**0.000179**	**0.000179**	**0.000179**
180-90	1.000000		**0.003454**	**0.000485**	**0.003439**	**0.000179**	**0.000179**	**0.000179**	**0.000179**
180-180	**0.002551**	**0.003454**		0.954279	1.000000	**0.000179**	**0.000179**	**0.000179**	**0.000179**
240-30	**0.000402**	**0.000485**	0.954279		0.954781	**0.000179**	**0.000179**	**0.000179**	**0.000179**
240-90	**0.002540**	**0.003439**	1.000000	0.954781		**0.000179**	**0.000179**	**0.000179**	**0.000179**
240-180	**0.000179**	**0.000179**	**0.000179**	**0.000179**	**0.000179**		0.054181	0.968570	**0.007716**
300-30	**0.000179**	**0.000179**	**0.000179**	**0.000179**	**0.000179**	0.054181		0.342749	**0.000190**
300-90	**0.000179**	**0.000179**	**0.000179**	**0.000179**	**0.000179**	0.968570	0.342749		**0.001220**
300-180	**0.000179**	**0.000179**	**0.000179**	**0.000179**	**0.000179**	**0.007716**	**0.000190**	**0.001220**	

Table A2. Two-way analysis of variance (ANOVA) with post-hoc Tukey test for VM content, a bold font signifies a statistically significant difference ($p < 0.05$).

Temp-Time	180-30	180-90	180-180	240-30	240-90	240-180	300-30	300-90	300-180
180-30		0.999655	**0.000177**	**0.000173**	**0.000173**	**0.000173**	**0.000173**	**0.000173**	**0.000173**
180-90	0.999655		**0.000193**	**0.000173**	**0.000173**	**0.000173**	**0.000173**	**0.000173**	**0.000173**
180-180	**0.000177**	**0.000193**		**0.000654**	**0.000174**	**0.000173**	**0.000173**	**0.000173**	**0.000173**
240-30	**0.000173**	**0.000173**	**0.000654**		0.136846	**0.000173**	**0.000173**	**0.000173**	**0.000173**
240-90	**0.000173**	**0.000173**	**0.000174**	0.136846		**0.000173**	**0.000173**	**0.000173**	**0.000173**
240-180	**0.000173**	**0.000173**	**0.000173**	**0.000173**	**0.000173**		**0.001330**	0.387176	0.053735
300-30	**0.000173**	**0.000173**	**0.000173**	**0.000173**	**0.000173**	**0.001330**		0.125784	**0.000174**
300-90	**0.000173**	**0.000173**	**0.000173**	**0.000173**	**0.000173**	0.387176	0.125784		**0.000614**
300-180	**0.000173**	**0.000173**	**0.000173**	**0.000173**	**0.000173**	0.053735	**0.000174**	**0.000614**	

Table A3. Two-way analysis of variance (ANOVA) with post-hoc Tukey test for FR, a bold font signifies a statistically significant difference ($p < 0.05$).

Temp-Time	180-30	180-90	180-180	240-30	240-90	240-180	300-30	300-90	300-180
180-30		1.000000	0.059948	**0.003027**	**0.004133**	**0.000179**	**0.000179**	**0.000179**	**0.000179**
180-90	1.000000		0.075922	**0.003854**	**0.005287**	**0.000179**	**0.000179**	**0.000179**	**0.000179**
180-180	0.059948	0.075922		0.827963	0.895906	**0.000179**	**0.000179**	**0.000179**	**0.000179**
240-30	**0.003027**	**0.003854**	0.827963		1.000000	**0.000179**	**0.000179**	**0.000179**	**0.000179**
240-90	**0.004133**	**0.005287**	0.895906	1.000000		**0.000179**	**0.000179**	**0.000179**	**0.000179**
240-180	**0.000179**	**0.000179**	**0.000179**	**0.000179**	**0.000179**		**0.000613**	0.377309	**0.000237**
300-30	**0.000179**	**0.000179**	**0.000179**	**0.000179**	**0.000179**	**0.000613**		**0.047955**	**0.000179**
300-90	**0.000179**	**0.000179**	**0.000179**	**0.000179**	**0.000179**	0.377309	**0.047955**		**0.000180**
300-180	**0.000179**	**0.000179**	**0.000179**	**0.000179**	**0.000179**	**0.000237**	**0.000179**	**0.000180**	

Preprints (www.preprints.org) | NOT PEER-REVIEWED | Posted: 19 July 2022 doi:10.20944/preprints202207.0277.v1

Table A4. Two-way analysis of variance (ANOVA) with post-hoc Tukey test for HHV, a bold font signifies a statistically significant difference ($p < 0.05$).

Temp-Time	180-30	180-90	180-180	240-30	240-90	240-180	300-30	300-90	300-180
180-30		0.079691	0.231818	**0.000179**	**0.000179**	**0.000179**	**0.000179**	**0.000179**	**0.000179**
180-90	0.079691		0.999219	**0.000179**	**0.000179**	**0.000179**	**0.000179**	**0.000179**	**0.000179**
180-180	0.231818	0.999219		**0.000179**	**0.000179**	**0.000179**	**0.000179**	**0.000179**	**0.000179**
240-30	**0.000179**	**0.000179**	**0.000179**		0.263009	**0.001506**	**0.000180**	**0.000179**	**0.000179**
240-90	**0.000179**	**0.000179**	**0.000179**	0.263009		0.200313	**0.000282**	**0.000179**	**0.000179**
240-180	**0.000179**	**0.000179**	**0.000179**	**0.001506**	0.200313		**0.026299**	**0.000190**	**0.000180**
300-30	**0.000179**	**0.000179**	**0.000179**	**0.000180**	**0.000282**	**0.026299**		**0.032128**	**0.001525**
300-90	**0.000179**	**0.000179**	**0.000179**	**0.000179**	**0.000179**	**0.000190**	**0.032128**		0.583350
300-180	**0.000179**	**0.000179**	**0.000179**	**0.000179**	**0.000179**	**0.000180**	**0.001525**	0.583350	

Table A5. Two-way analysis of variance (ANOVA) with post-hoc Tukey test for EDr, a bold font signifies a statistically significant difference ($p < 0.05$).

Temp-Time	180-30	180-90	180-180	240-30	240-90	240-180	300-30	300-90	300-180
180-30		0.079691	0.231818	**0.000179**	**0.000179**	**0.000179**	**0.000179**	**0.000179**	**0.000179**
180-90	0.079691		0.999219	**0.000179**	**0.000179**	**0.000179**	**0.000179**	**0.000179**	**0.000179**
180-180	0.231818	0.999219		**0.000179**	**0.000179**	**0.000179**	**0.000179**	**0.000179**	**0.000179**
240-30	**0.000179**	**0.000179**	**0.000179**		0.263009	**0.001506**	**0.000180**	**0.000179**	**0.000179**
240-90	**0.000179**	**0.000179**	**0.000179**	0.263009		0.200313	**0.000282**	**0.000179**	**0.000179**
240-180	**0.000179**	**0.000179**	**0.000179**	**0.001506**	0.200313		**0.026299**	**0.000190**	**0.000180**
300-30	**0.000179**	**0.000179**	**0.000179**	**0.000180**	**0.000282**	**0.026299**		**0.032128**	**0.001525**
300-90	**0.000179**	**0.000179**	**0.000179**	**0.000179**	**0.000179**	**0.000190**	**0.032128**		0.583350
300-180	**0.000179**	**0.000179**	**0.000179**	**0.000179**	**0.000179**	**0.000180**	**0.001525**	0.583350	

Table A6. Two-way analysis of variance (ANOVA) with post-hoc Tukey test for EG, a bold font signifies a statistically significant difference ($p < 0.05$).

Temp-Time	180-30	180-90	180-180	240-30	240-90	240-180	300-30	300-90	300-180
180-30		0.532195	0.297506	**0.000969**	**0.004063**	**0.002547**	**0.014402**	**0.007121**	**0.007255**
180-90	0.532195		0.999929	**0.049147**	0.199114	0.132063	0.494994	0.310076	0.226234
180-180	0.297506	0.999929		0.112451	0.387730	0.274307	0.756693	0.548802	0.404615
240-30	**0.000969**	**0.049147**	0.112451		0.996028	0.999716	0.873862	0.971603	0.999864
240-90	**0.004063**	0.199114	0.387730	0.996028		0.999999	0.998990	0.999998	1.000000
240-180	**0.002547**	0.132063	0.274307	0.999716	0.999999		0.990973	0.999748	1.000000
300-30	**0.014402**	0.494994	0.756693	0.873862	0.998990	0.990973		0.999988	0.995865
300-90	**0.007121**	0.310076	0.548802	0.971603	0.999998	0.999748	0.999988		0.999900
300-180	**0.007255**	0.226234	0.404615	0.999864	1.000000	1.000000	0.995865	0.999900	

Preprints (www.preprints.org) | NOT PEER-REVIEWED | Posted: 19 July 2022 doi:10.20944/preprints202207.0277.v1

Table A7. Two-way analysis of variance (ANOVA) with post-hoc Tukey test for LHV, a bold font signifies a statistically significant difference ($p < 0.05$).

Temp-Time	180-30	180-90	180-180	240-30	240-90	240-180	300-30	300-90	300-180
180-30		0.998134	0.894723	0.881308	0.791296	0.775648	0.529865	0.491547	0.999995
180-90	0.998134		0.998684	0.998092	0.990020	0.987744	0.901792	0.877401	0.978751
180-180	0.894723	0.998684		1.000000	1.000000	0.999999	0.998487	0.997120	0.746110
240-30	0.881308	0.998092	1.000000		1.000000	1.000000	0.998960	0.997944	0.726189
240-90	0.791296	0.990020	1.000000	1.000000		1.000000	0.999928	0.999802	0.609648
240-180	0.775648	0.987744	0.999999	1.000000	1.000000		0.999957	0.999873	0.591591
300-30	0.529865	0.901792	0.998487	0.998960	0.999928	0.999957		1.000000	0.354686
300-90	0.491547	0.877401	0.997120	0.997944	0.999802	0.999873	1.000000		0.323264
300-180	0.999995	0.978751	0.746110	0.726189	0.609648	0.591591	0.354686	0.323264	

Table A8. Two-way analysis of variance (ANOVA) with post-hoc Tukey test for Eu, a bold font signifies a statistically significant difference ($p < 0.05$).

Temp-Time	180-30	180-90	180-180	240-30	240-90	240-180	300-30	300-90	300-180
180-30		0.999097	0.992207	0.914849	0.825810	**0.029185**	**0.000656**	**0.000178**	**0.000173**
180-90	0.999097		1.000000	0.998549	0.990130	0.099527	**0.002034**	**0.000201**	**0.000173**
180-180	0.992207	1.000000		0.999933	0.998715	0.151170	**0.003218**	**0.000222**	**0.000174**
240-30	0.914849	0.998549	0.999933		1.000000	0.310124	**0.007899**	**0.000283**	**0.000174**
240-90	0.825810	0.990130	0.998715	1.000000		0.421561	**0.012434**	**0.000344**	**0.000174**
240-180	**0.029185**	0.099527	0.151170	0.310124	0.421561		0.588943	**0.019172**	**0.000378**
300-30	**0.000656**	**0.002034**	**0.003218**	**0.007899**	**0.012434**	0.588943		0.543987	**0.012768**
300-90	**0.000178**	**0.000201**	**0.000222**	**0.000283**	**0.000344**	**0.019172**	0.543987		0.470804
300-180	**0.000173**	**0.000173**	**0.000174**	**0.000174**	**0.000174**	**0.000378**	**0.012768**	0.470804	

Table A9. Two-way analysis of variance (ANOVA) with post-hoc Tukey test for Eg, a bold font signifies a statistically significant difference ($p < 0.05$).

Temp-Time	180-30	180-90	180-180	240-30	240-90	240-180	300-30	300-90	300-180
180-30		0.998482	0.979937	0.978842	0.959880	0.060731	**0.001846**	**0.000226**	**0.000174**
180-90	0.998482		0.999994	0.999992	0.999921	0.207517	**0.007184**	**0.000369**	**0.000176**
180-180	0.979937	0.999994		1.000000	1.000000	0.342616	**0.014010**	**0.000561**	**0.000179**
240-30	0.978842	0.999992	1.000000		1.000000	0.347012	**0.014269**	**0.000568**	**0.000179**
240-90	0.959880	0.999921	1.000000	1.000000		0.408394	**0.018199**	**0.000681**	**0.000181**
240-180	0.060731	0.207517	0.342616	0.347012	0.408394		0.714569	0.056654	**0.001370**
300-30	**0.001846**	**0.007184**	**0.014010**	**0.014269**	**0.018199**	0.714569		0.741379	**0.044874**
300-90	**0.000226**	**0.000369**	**0.000561**	**0.000568**	**0.000681**	0.056654	0.741379		0.644241
300-180	**0.000174**	**0.000176**	**0.000179**	**0.000179**	**0.000181**	**0.001370**	**0.044874**	0.644241	

Preprints (www.preprints.org) | NOT PEER-REVIEWED | Posted: 19 July 2022 doi:10.20944/preprints202207.0277.v1

Table A10. Two-way analysis of variance (ANOVA) with post-hoc Tukey test for AC, a bold font signifies a statistically significant difference ($p < 0.05$).

Temp-Time	180-30	180-90	180-180	240-30	240-90	240-180	300-30	300-90	300-180
180-30		0.999343	**0.001621**	**0.000179**	**0.000179**	**0.000179**	**0.000179**	**0.000179**	**0.000179**
180-90	0.999343		**0.005126**	**0.000179**	**0.000179**	**0.000179**	**0.000179**	**0.000179**	**0.000179**
180-180	**0.001621**	**0.005126**		**0.000253**	**0.000179**	**0.000179**	**0.000179**	**0.000179**	**0.000179**
240-30	**0.000179**	**0.000179**	**0.000253**		**0.000978**	**0.000236**	0.060754	**0.003446**	**0.000304**
240-90	**0.000179**	**0.000179**	**0.000179**	**0.000978**		0.913416	0.470757	0.998303	0.833690
240-180	**0.000179**	**0.000179**	**0.000179**	**0.000236**	0.913416		0.055773	0.559710	0.999991
300-30	**0.000179**	**0.000179**	**0.000179**	0.060754	0.470757	0.055773		0.855566	0.058638
300-90	**0.000179**	**0.000179**	**0.000179**	**0.003446**	0.998303	0.559710	0.855566		0.484494
300-180	**0.000179**	**0.000179**	**0.000179**	**0.000304**	0.833690	0.999991	0.058638	0.484494	

Table A11. Two-way analysis of variance (ANOVA) with post-hoc Tukey test for C, a bold font signifies a statistically significant difference ($p < 0.05$).

Temp-Time	180-30	180-90	180-180	240-30	240-90	240-180	300-30	300-90	300-180
180-30		0.227399	**0.027356**	**0.000198**	**0.000180**	**0.000179**	**0.000179**	**0.000179**	**0.000179**
180-90	0.227399		0.953385	**0.005171**	**0.000360**	**0.000195**	**0.000179**	**0.000179**	**0.000179**
180-180	**0.027356**	0.953385		0.051131	**0.002111**	**0.000380**	**0.000180**	**0.000179**	**0.000179**
240-30	**0.000198**	**0.005171**	0.051131		0.774741	0.201874	**0.001880**	**0.000217**	**0.000258**
240-90	**0.000180**	**0.000360**	**0.002111**	0.774741		0.963841	**0.045488**	**0.001348**	**0.001602**
240-180	**0.000179**	**0.000195**	**0.000380**	0.201874	0.963841		0.312711	**0.011444**	**0.010982**
300-30	**0.000179**	**0.000179**	**0.000180**	**0.001880**	**0.045488**	0.312711		0.671354	0.504387
300-90	**0.000179**	**0.000179**	**0.000179**	**0.000217**	**0.001348**	**0.011444**	0.671354		0.999892
300-180	**0.000179**	**0.000179**	**0.000179**	**0.000258**	**0.001602**	**0.010982**	0.504387	0.999892	

Table A12. Two-way analysis of variance (ANOVA) with post-hoc Tukey test for H, a bold font signifies a statistically significant difference ($p < 0.05$).

Temp-Time	180-30	180-90	180-180	240-30	240-90	240-180	300-30	300-90	300-180
180-30		0.982533	**0.001958**	**0.000225**	**0.000179**	**0.000179**	**0.000179**	**0.000179**	**0.000179**
180-90	0.982533		**0.013231**	**0.000551**	**0.000180**	**0.000179**	**0.000179**	**0.000179**	**0.000179**
180-180	**0.001958**	**0.013231**		0.711229	**0.005572**	**0.000477**	**0.000185**	**0.000182**	**0.000182**
240-30	**0.000225**	**0.000551**	0.711229		0.157640	**0.010655**	**0.000419**	**0.000305**	**0.000267**
240-90	**0.000179**	**0.000180**	**0.005572**	0.157640		0.874698	0.079903	**0.043027**	**0.016201**
240-180	**0.000179**	**0.000179**	**0.000477**	**0.010655**	0.874698		0.647226	0.454186	0.174881
300-30	**0.000179**	**0.000179**	**0.000185**	**0.000419**	0.079903	0.647226		0.999993	0.951913
300-90	**0.000179**	**0.000179**	**0.000182**	**0.000305**	**0.043027**	0.454186	0.999993		0.991288
300-180	**0.000179**	**0.000179**	**0.000182**	**0.000267**	**0.016201**	0.174881	0.951913	0.991288	

Preprints (www.preprints.org) | NOT PEER-REVIEWED | Posted: 19 July 2022 doi:10.20944/preprints202207.0277.v1

Table A13. Two-way analysis of variance (ANOVA) with post-hoc Tukey test for N, a bold font signifies a statistically significant difference ($p < 0.05$).

Temp-Time	180-30	180-90	180-180	240-30	240-90	240-180	300-30	300-90	300-180
180-30		0.992151	0.749174	**0.000181**	**0.000180**	**0.000179**	**0.000179**	**0.000179**	**0.000179**
180-90	0.992151		0.994697	**0.000191**	**0.000182**	**0.000180**	**0.000179**	**0.000179**	**0.000180**
180-180	0.749174	0.994697		**0.000261**	**0.000194**	**0.000183**	**0.000180**	**0.000180**	**0.000181**
240-30	**0.000181**	**0.000191**	**0.000261**		0.997828	0.920371	0.455796	0.271316	0.288165
240-90	**0.000180**	**0.000182**	**0.000194**	0.997828		0.999528	0.855040	0.655387	0.634350
240-180	**0.000179**	**0.000180**	**0.000183**	0.920371	0.999528		0.990572	0.927863	0.896584
300-30	**0.000179**	**0.000179**	**0.000180**	0.455796	0.855040	0.990572		0.999981	0.999587
300-90	**0.000179**	**0.000179**	**0.000180**	0.271316	0.655387	0.927863	0.999981		1.000000
300-180	**0.000179**	**0.000180**	**0.000181**	0.288165	0.634350	0.896584	0.999587	1.000000	

Table A14. Two-way analysis of variance (ANOVA) with post-hoc Tukey test for S, a bold font signifies a statistically significant difference ($p < 0.05$).

Temp-Time	180-30	180-90	180-180	240-30	240-90	240-180	300-30	300-90	300-180
180-30		0.637097	0.999163	0.315181	0.396858	0.920547	0.757102	0.920547	0.999774
180-90	0.637097		0.932724	0.999490	0.999958	0.999490	1.000000	0.999490	0.955744
180-180	0.999163	0.932724		0.661863	0.757102	0.998679	0.975403	0.998679	1.000000
240-30	0.315181	0.999490	0.661863		1.000000	0.953319	0.995645	0.953319	0.751432
240-90	0.396858	0.999958	0.757102	1.000000		0.980704	0.999163	0.980704	0.827812
240-180	0.920547	0.999490	0.998679	0.953319	0.980704		0.999981	1.000000	0.999078
300-30	0.757102	1.000000	0.975403	0.995645	0.999163	0.999981		0.999981	0.984060
300-90	0.920547	0.999490	0.998679	0.953319	0.980704	1.000000	0.999981		0.999078
300-180	0.999774	0.955744	1.000000	0.751432	0.827812	0.999078	0.984060	0.999078	

Table A15. Two-way analysis of variance (ANOVA) with post-hoc Tukey test for O, a bold font signifies a statistically significant difference ($p < 0.05$).

Temp-Time	180-30	180-90	180-180	240-30	240-90	240-180	300-30	300-90	300-180
180-30		0.211682	**0.000410**	**0.000179**	**0.000179**	**0.000179**	**0.000179**	**0.000179**	**0.000179**
180-90	0.211682		0.055413	**0.000180**	**0.000179**	**0.000179**	**0.000179**	**0.000179**	**0.000179**
180-180	**0.000410**	0.055413		**0.000930**	**0.000179**	**0.000179**	**0.000179**	**0.000179**	**0.000179**
240-30	**0.000179**	**0.000180**	**0.000930**		**0.004665**	**0.000386**	**0.000624**	**0.000181**	**0.000180**
240-90	**0.000179**	**0.000179**	**0.000179**	**0.004665**		0.834830	0.960509	**0.042917**	**0.003594**
240-180	**0.000179**	**0.000179**	**0.000179**	**0.000386**	0.834830		0.999979	0.506188	0.051070
300-30	**0.000179**	**0.000179**	**0.000179**	**0.000624**	0.960509	0.999979		0.306933	**0.026388**
300-90	**0.000179**	**0.000179**	**0.000179**	**0.000181**	**0.042917**	0.506188	0.306933		0.769687
300-180	**0.000179**	**0.000179**	**0.000179**	**0.000180**	**0.003594**	0.051070	**0.026388**	0.769687	

Preprints (www.preprints.org) | NOT PEER-REVIEWED | Posted: 19 July 2022 doi:10.20944/preprints202207.0277.v1

Table A16. Two-way analysis of variance (ANOVA) with post-hoc Tukey test for MY, a bold font signifies a statistically significant difference ($p < 0.05$).

Temp-Time	180-30	180-90	180-180	240-30	240-90	240-180	300-30	300-90	300-180
180-30		0.999311	0.452863	0.984550	1.000000	0.994656	0.125802	**0.039934**	0.085584
180-90	0.999311		0.802487	0.999988	0.993907	0.873134	**0.040730**	**0.012082**	**0.030419**
180-180	0.452863	0.802487		0.939617	0.336426	0.130783	**0.001864**	**0.000656**	**0.001932**
240-30	0.984550	0.999988	0.939617		0.948429	0.692900	**0.020329**	**0.005975**	**0.016267**
240-90	1.000000	0.993907	0.336426	0.948429		0.999432	0.184553	0.061290	0.122765
240-180	0.994656	0.873134	0.130783	0.692900	0.999432		0.440551	0.176630	0.291614
300-30	0.125802	**0.040730**	**0.001864**	**0.020329**	0.184553	0.440551		0.999223	0.999732
300-90	**0.039934**	**0.012082**	**0.000656**	**0.005975**	0.061290	0.176630	0.999223		1.000000
300-180	0.085584	**0.030419**	**0.001932**	**0.016267**	0.122765	0.291614	0.999732	1.000000	

Table A17. Two-way analysis of variance (ANOVA) with post-hoc Tukey test for EY, a bold font signifies a statistically significant difference ($p < 0.05$).

Temp-Time	180-30	180-90	180-180	240-30	240-90	240-180	300-30	300-90	300-180
180-30		0.985620	0.413447	0.261108	0.752136	0.895446	0.998506	0.971773	0.996339
180-90	0.985620		0.915607	0.775833	0.997661	0.999960	0.776006	0.550693	0.779922
180-180	0.413447	0.915607		0.999994	0.999482	0.990366	0.146593	0.073108	0.187361
240-30	0.261108	0.775833	0.999994		0.989291	0.941198	0.082249	**0.039490**	0.113846
240-90	0.752136	0.997661	0.999482	0.989291		0.999996	0.364845	0.203647	0.408015
240-180	0.895446	0.999960	0.990366	0.941198	0.999996		0.535524	0.326783	0.565892
300-30	0.998506	0.776006	0.146593	0.082249	0.364845	0.535524		0.999976	1.000000
300-90	0.971773	0.550693	0.073108	**0.039490**	0.203647	0.326783	0.999976		1.000000
300-180	0.996339	0.779922	0.187361	0.113846	0.408015	0.565892	1.000000	1.000000	

Preprints (www.preprints.org) | NOT PEER-REVIEWED | Posted: 19 July 2022 doi:10.20944/preprints202207.0277.v1

Appendix B

Appendix B contains graphs presenting temperature and pressure patterns during the HTC process with different parameters.

Figure B1, Figure B2 and Figure B3 present the temperature and pressure patterns for the HTC process performed at 180 °C, 30, 90 and 180 min, respectively.

Figure B4, Figure B5 and Figure B6 present the temperature and pressure patterns for the HTC process performed at 240 °C, 30, 90 and 180 min, respectively.

Figure B7 and Figure B8 present the temperature and pressure patterns for the HTC process performed at 300 °C, 30, 90, respectively.

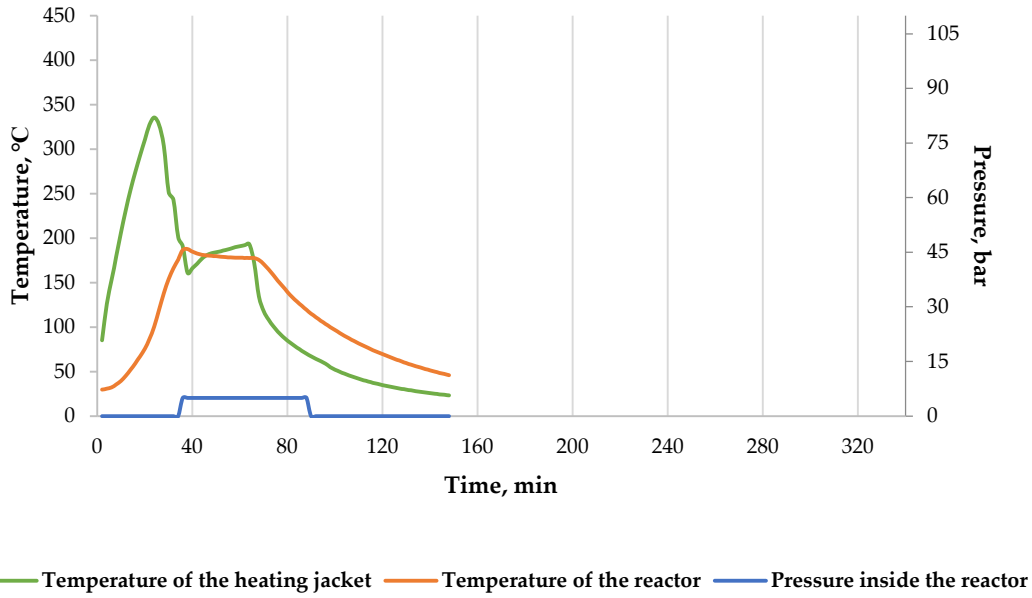

Figure B1. Temperature and pressure patterns during the process at 180 °C in 30 min.

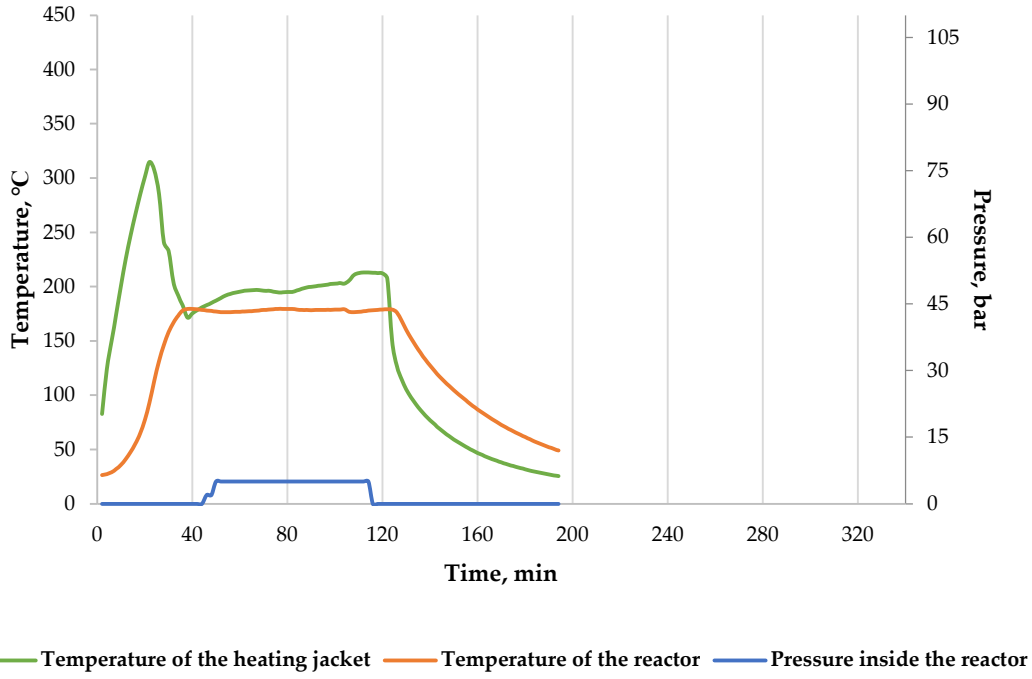

Figure B2. Temperature and pressure patterns during the process at 180 °C in 90 min.

Preprints (www.preprints.org) | NOT PEER-REVIEWED | Posted: 19 July 2022 doi:10.20944/preprints202207.0277.v1

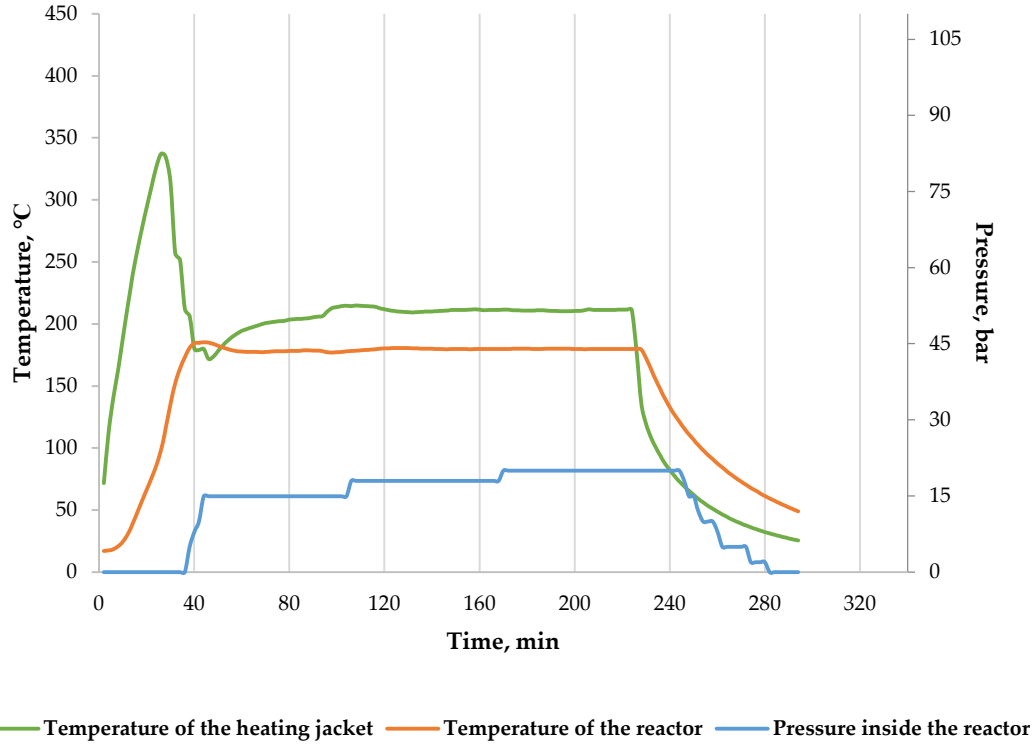

Figure B3. Temperature and pressure patterns during the process at 180 °C in 180 min.

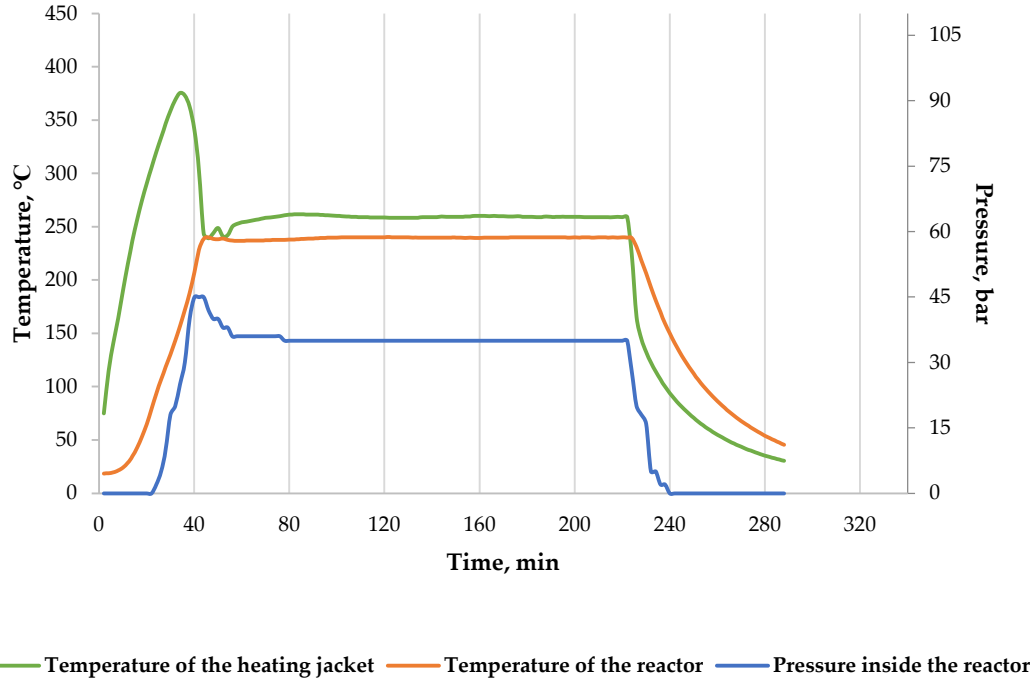

Figure B4. Temperature and pressure patterns during the process at 240 °C in 30 min.

Preprints (www.preprints.org) | NOT PEER-REVIEWED | Posted: 19 July 2022 doi:10.20944/preprints202207.0277.v1

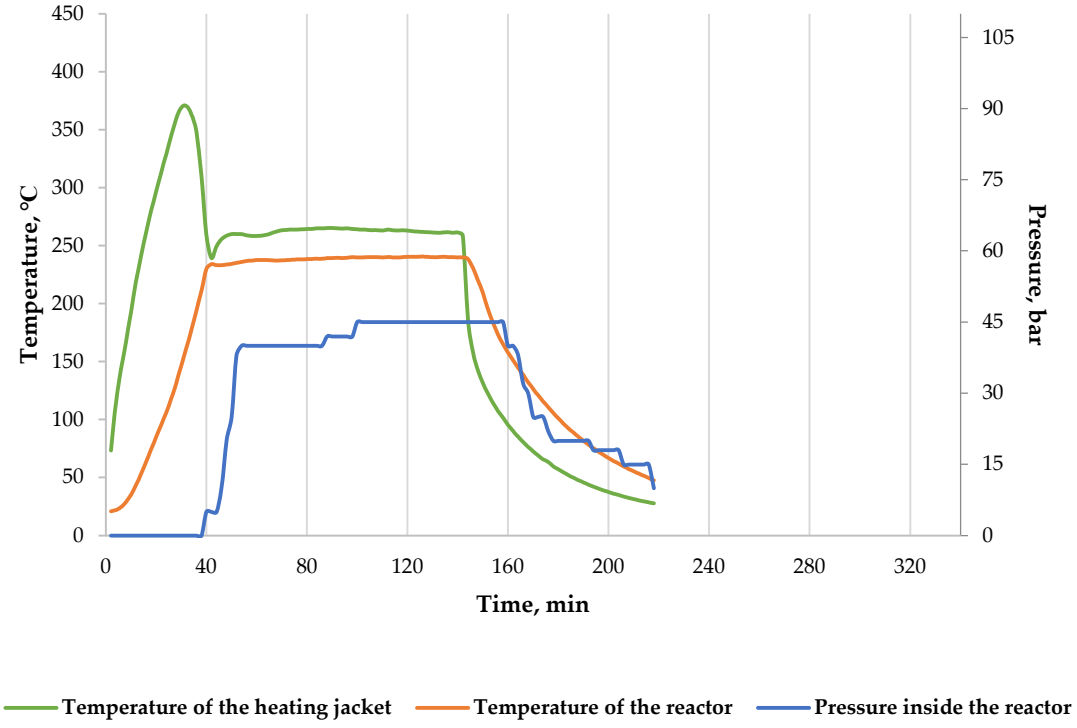

Figure B5. Temperature and pressure patterns during the process at 240 °C in 90 min.

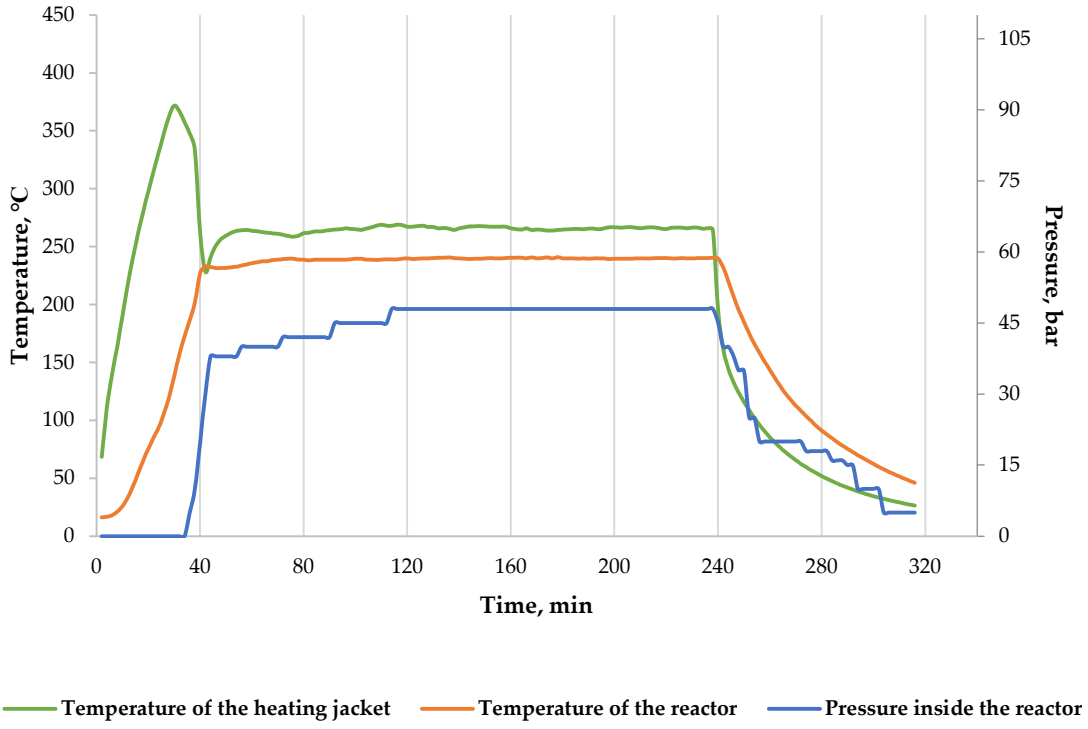

Figure B6. Temperature and pressure patterns during the process at 240 °C in 180 min.

Preprints (www.preprints.org) | NOT PEER-REVIEWED | Posted: 19 July 2022 doi:10.20944/preprints202207.0277.v1

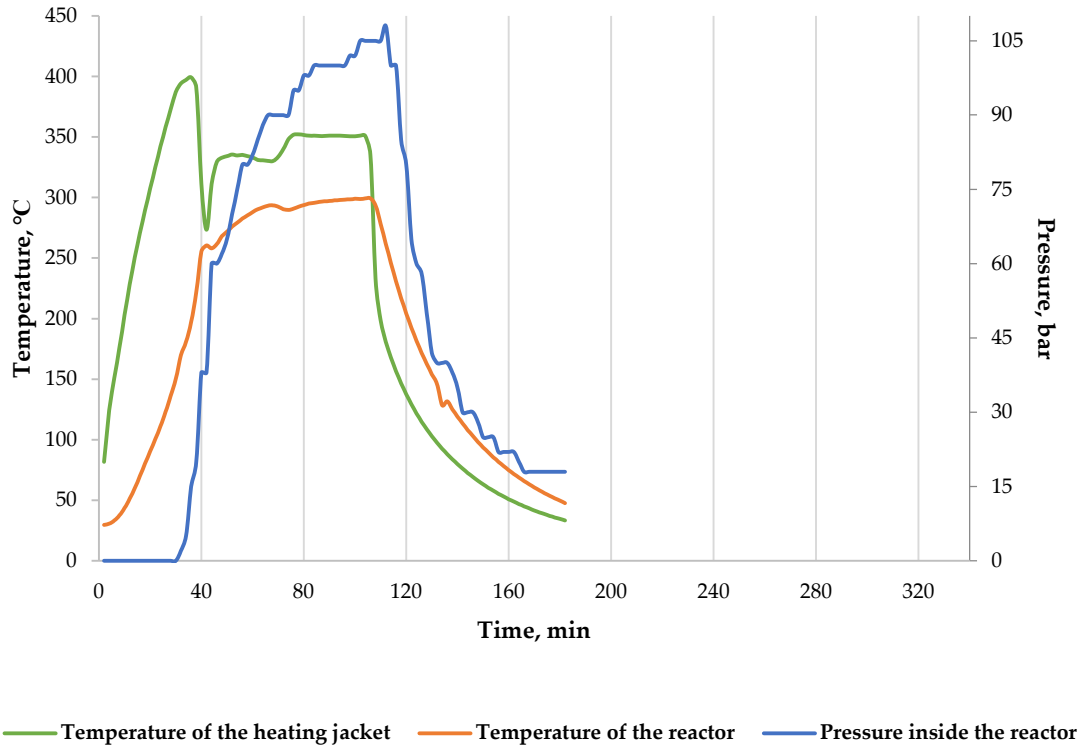

Figure B7. Temperature and pressure patterns during the process at 300 °C in 30 min.

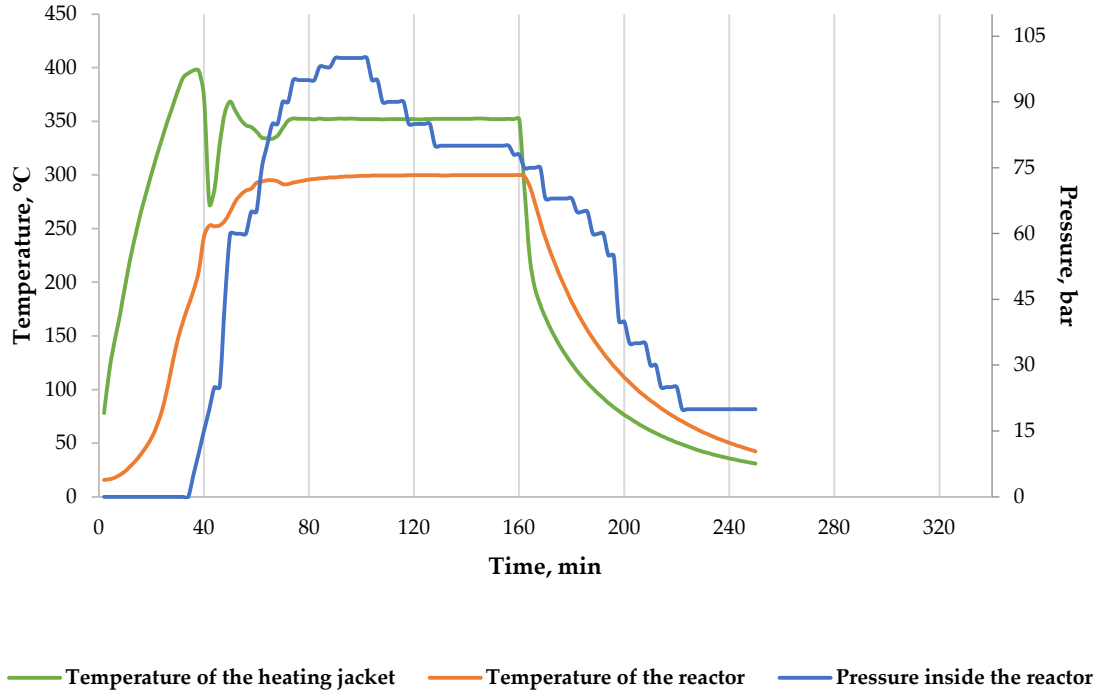

Figure B8. Temperature and pressure patterns during the process at 300 °C in 90 min.

References

1. A.R. Seidavi, H. Zaker-Esteghamati, C.G. Scanes, Present and potential impacts of waste from poultry production on the environment, Worlds. Poult. Sci. J. 75 (2019) 29–42. https://doi.org/10.1017/S0043933918000922
2. J.T. Sims, Agricultural and Environmental Issues in the Management of Poultry Wastes: Recent Innovations and Long-Term Challenges, ACS Symp. Ser. 668 (1997) 72–90. https://doi.org/10.1021/bk-1997-0668.ch006.
3. M. Tańczuk, R. Junga, A. Kolasa-Więcek, P. Niemiec, Assessment of the energy potential of chicken manure in Poland, Energies. 12 (2019). https://doi.org/10.3390/en12071244.
4. M. Tańczuk, R. Junga, S. Werle, M. Chabiński, Ziółkowski, Experimental analysis of the fixed bed gasification process of the mixtures of the chicken manure with biomass, Renew. Energy. 136 (2019) 1055–1063. https://doi.org/10.1016/j.renene.2017.05.074.
5. L. Jurgutis, A. Slepetiene, J. Volungevicius, K. Amaleviciute-Volunge, Biogas production from chicken manure at different organic loading rates in a mesophilic full scale anaerobic digestion plant, Biomass and Bioenergy. 141 (2020) 105693. https://doi.org/10.1016/j.biombioe.2020.105693.
6. D. Bhatt, A. Shrestha, R.K. Dahal, B. Acharya, P. Basu, R. MacEwen, Hydrothermal carbonization of biosolids from Waste water treatment plant, Energies. 11 (2018) 1–10. https://doi.org/10.3390/en11092286.
7. F. Santos Dalólio, J.N. da Silva, A.C. Carneiro de Oliveira, I. de F. Ferreira Tinôco, R. Christiam Barbosa, M. de O. Resende, L.F. Teixeira Albino, S. Teixeira Coelho, Poultry litter as biomass energy: A review and future perspectives, Renew. Sustain. Energy Rev. 76 (2017) 941–949. https://doi.org/10.1016/j.rser.2017.03.104.
8. W.A. Rasaq, M. Golonka, M. Scholz, A. Białowiec, Opportunities and challenges of high-pressure fast pyrolysis of biomass: A review, Energies. 14 (2021) 1–20. https://doi.org/10.3390/en14175426.
9. A. Zabaniotou, D. Rovas, M.K. Delivand, M. Francavilla, A. Libutti, A.R. Cammerino, M. Monteleone, Conceptual vision of bioenergy sector development in Mediterranean regions based on decentralized thermochemical systems, Sustain. Energy Technol. Assessments. 23 (2017) 33–47. https://doi.org/10.1016/j.seta.2017.09.006.
10. N. Bhatnagar, D. Ryan, R. Murphy, A.M. Enright, A comprehensive review of green policy, anaerobic digestion of animal manure and chicken litter feedstock potential – Global and Irish perspective, Renew. Sustain. Energy Rev. 154 (2022) 111884. https://doi.org/10.1016/j.rser.2021.111884.
11. R. Isemin, N. Muratova, S. Kuzmin, D. Klimov, V. Kokh-Tatarenko, A. Mikhalev, O. Milovanov, A. Dalibard, O.A. Ibitowa, M. Nowotny, M. Brulé, F. Tabet, B. Rogge, Characteristics of Hydrochar and Liquid Products Obtained by Hydrothermal Carbonization and Wet Torrefaction of Poultry Litter in Mixture with Wood Sawdust, Processes. 9 (2021) 1–10. https://doi.org/10.3390/pr9112082.
12. A.R. El Boushy, G.J. Klaassen, E.H. Ketelaars, Biological Conversion of Poultry and Animal Waste to a Feedstuff for Poultry, Worlds. Poult. Sci. J. 41 (1985) 133–145. https://doi.org/10.1079/WPS19850012.
13. A. Urbanowska, M. Kabsch-Korbutowicz, C. Aragon-Briceño, M. Wnukowski, A. Pożarlik, L. Niedzwiecki, M. Baranowski, M. Czerep, P. Seruga, H. Pawlak-Kruczek, E. Bramer, G. Brem, Cascade membrane system for separation of water and organics from liquid by-products of htc of the agricultural digestate—evaluation of performance, Energies. 14 (2021). https://doi.org/10.3390/en14164752.
14. P. Taylor, A. Demirbas, Production of Gasoline and Diesel Fuels from Bio- materials, (2007) 753–760. https://doi.org/10.1080/00908310500281288.
15. A. Abdalazeez, T. Li, W. Wang, S. Abuelgasim, A brief review of CO2utilization for alkali carbonate gasification and biomass/coal co-gasification: Reactivity, products and process, J. CO2 Util. 43 (2021) 101370. https://doi.org/10.1016/j.jcou.2020.101370.
16. M.H. Marzbali, S. Kundu, P. Halder, S. Patel, I.G. Hakeem, J. Paz-Ferreiro, S. Madapusi, A. Surapaneni, K. Shah, Wet organic waste treatment via hydrothermal processing: A critical review, Chemosphere. 279 (2021) 130557. https://doi.org/10.1016/j.chemosphere.2021.130557.
17. T. Wang, Y. Zhai, Y. Zhu, C. Li, G. Zeng, A review of the hydrothermal carbonization of biomass waste for hydrochar formation: Process conditions, fundamentals, and physicochemical properties, Renew. Sustain. Energy Rev. 90 (2018) 223–247. https://doi.org/10.1016/j.rser.2018.03.071.
18. G. Ischia, L. Fiori, Hydrothermal Carbonization of Organic Waste and Biomass: A Review on Process, Reactor, and Plant Modeling, Waste and Biomass Valorization. 12 (2021) 2797–2824. https://doi.org/10.1007/s12649-020-01255-3.
19. A.L. Pauline, K. Joseph, Hydrothermal carbonization of organic wastes to carbonaceous solid fuel – A review of mechanisms and process parameters, Fuel. 279 (2020) 118472. https://doi.org/10.1016/j.fuel.2020.118472.
20. M. Heidari, A. Dutta, B. Acharya, S. Mahmud, A review of the current knowledge and challenges of hydrothermal carbonization for biomass conversion, J. Energy Inst. 92 (2019) 1779–1799. https://doi.org/10.1016/j.joei.2018.12.003.
21. Y. Lin, X. Ma, X. Peng, Z. Yu, A Mechanism Study on Hydrothermal Carbonization of Waste Textile, Energy and Fuels. 30 (2016) 7746–7754. https://doi.org/10.1021/acs.energyfuels.6b01365.
22. D. Lachos-Perez, P. César Torres-Mayanga, E.R. Abaide, G.L. Zabot, F. De Castilhos, Hydrothermal carbonization and Liquefaction: differences, progress, challenges, and opportunities, Bioresour. Technol. 343 (2022) 126084. https://doi.org/10.1016/j.biortech.2021.126084.
23. D.V.S.R. Vinu, Effects of Biomass Particle Size on Slow Pyrolysis Kinetics and Fast Pyrolysis Product Distribution, Waste and Biomass Valorization. 0 (2017) 1–13. https://doi.org/10.1007/s12649-016-9815-7.

24. V. Mau, A. Gross, Energy conversion and gas emissions from production and combustion of poultry-litter-derived hydrochar and biochar, Appl. Energy. 213 (2018) 510–519. https://doi.org/10.1016/j.apenergy.2017.11.033.
25. S. Zhou, H. Liang, L. Han, G. Huang, Z. Yang, The influence of manure feedstock, slow pyrolysis, and hydrothermal temperature on manure thermochemical and combustion properties, Waste Manag. 88 (2019) 85–95. https://doi.org/10.1016/j.wasman.2019.03.025.
26. B.M. Ghanim, D.S. Pandey, W. Kwapinski, J.J. Leahy, Hydrothermal carbonisation of poultry litter: Effects of treatment temperature and residence time on yields and chemical properties of hydrochars, Bioresour. Technol. 216 (2016) 373–380. https://doi.org/10.1016/j.biortech.2016.05.087.
27. P. Stępień, M. Serowik, J.A. Koziel, A. Białowiec, Waste to carbon energy demand model and data based on the TGA and DSC analysis of individual MSW components, Data. 4 (2019) 1–6. https://doi.org/10.3390/data4020053.
28. H. Zhou, Y.Q. Long, A.H. Meng, Q.H. Li, Y.G. Zhang, Thermogravimetric characteristics of typical municipal solid waste fractions during co-pyrolysis, Waste Manag. 38 (2015) 194–200. https://doi.org/10.1016/j.wasman.2014.09.027.
29. LPP Equipment sp. z o., High pressure reactors, (2022) 1–2. https://doi.org/https://www.lpp-equipment.pl/en/products/reactors/pressure/high-pressure.
30. K. Świechowski, M. Liszewski, P. Babelewski, J. A. Koziel, and A. Białowiec, "Fuel properties of torrefied biomass from pruning of oxytree," Data, vol. 4, no. 2, pp. 2–11, 2019, doi: 10.3390/data4020055.
31. L. D. M. Torquato, P. M. Crnkovic, C. A. Ribeiro, and M. S. Crespi, "New approach for proximate analysis by thermogravimetry using CO2 atmosphere: Validation and application to different biomasses," *J. Therm. Anal. Calorim.*, vol. 128, no. 1, pp. 1–14, 2017, doi: 10.1007/s10973-016-5882-z.
32. PN-EN 15935:2022-01 Standard, *Waste Characteristics. determination of loss on ignition of sludge, treated biowaste, soil and waste*. 2022, p. 15935.
33. PN EN ISO 18125:2017-07, *Solid Biofuels—Determination of Calorific Value.* 2021, p. 18125.
34. P. Devi, A. K. Saroha, Effect of pyrolysis temperature on polycyclic aromatic hydrocarbons toxicity and sorption behaviour of biochars prepared by pyrolysis of paper mill effluent treatment plant sludge, Bioresour. Technol. 192 (2015) 312–320. https://doi.org/10.1016/j.biortech.2015.05.084
35. PN-EN ISO 16948: 2015-07 Standard, *Solid biofuels - Determination of total carbon, hydrogen and nitrogen content*. 2015, p. 16948.
36. P. Stępień, J. Pulka, M. Serowik, and A. Białowiec, "Thermogravimetric and Calorimetric Characteristics of Alternative Fuel in Terms of Its Use in Low-Temperature Pyrolysis," Waste and Biomass Valorization, vol. 10, no. 6, pp. 1669–1677, 2019, doi: 10.1007/s12649-017-0169-6.
37. S. Cardona, L.J. Gallego, V. Valencia, E. Martínez, L.A. Rios, Torrefaction of eucalyptus-tree residues: A new method for energy and mass balances of the process with the best torrefaction conditions, Sustain. Energy Technol. Assessments. 31 (2019) 17–24. https://doi.org/10.1016/j.seta.2018.11.002.
38. Q. Li, S. Zhang, M. Gholizadeh, X. Hu, X. Yuan, B. Sarkar, M. Vithanage, O. Mašek, Y.S. Ok, Co-hydrothermal carbonization of swine and chicken manure: Influence of cross-interaction on hydrochar and liquid characteristics, Sci. Total Environ. 786 (2021). https://doi.org/10.1016/j.scitotenv.2021.147381.
39. Z. Yıldız, N. Kaya, Y. Topcu, H. Uzun, Pyrolysis and optimization of chicken manure wastes in fluidized bed reactor: CO2 capture in activated bio-chars, Process Saf. Environ. Prot. 130 (2019) 297–305. https://doi.org/10.1016/j.psep.2019.08.011.
40. M.S. Hussein, K.G. Burra, R.S. Amano, A.K. Gupta, Temperature and gasifying media effects on chicken manure pyrolysis and gasification, Fuel. 202 (2017) 36–45. https://doi.org/10.1016/j.fuel.2017.04.017.
41. X. Yang, K. Kang, L. Qiu, L. Zhao, R. Sun, Effects of carbonization conditions on the yield and fixed carbon content of biochar from pruned apple tree branches, Renew. Energy. 146 (2020) 1691–1699. https://doi.org/10.1016/j.renene.2019.07.148.
42. D. Perondi, P. Poletto, D. Restelatto, C. Manera, J.P. Silva, J. Junges, G.C. Collazzo, A. Dettmer, M. Godinho, A.C.F. Vilela, Steam gasification of poultry litter biochar for bio-syngas production, Process Saf. Environ. Prot. 109 (2017) 478–488. https://doi.org/10.1016/j.psep.2017.04.029.
43. M. Kozak, Rozwój metod oznaczania siarki w paliwach i w komponentach paliw technikami spektrometrii atomowej, Nafta-Gaz. 74 (2018) 619–624. https://doi.org/10.18668/ng.2018.08.08.
44. P. Basu, Biomass Gasification, Pyrolysis and Torrefaction: Practical Design and Theory, in: Chapter 11, 2018: pp. 393–413. https://doi.org/10.1016/B978-0-12-812992-0/00011-X.
45. R. Muthu Dinesh Kumar, R. Anand, Production of biofuel from biomass downdraft gasification and its applications, Elsevier Ltd, 2019. https://doi.org/10.1016/B978-0-08-102791-2.00005-2.
46. F. Li, Z. Jiang, W. Ji, Y. Chen, J. Ma, X. Gui, J. Zhao, C. Zhou, Effects of hydrothermal carbonization temperature on carbon retention, stability, and properties of animal manure-derived hydrochar, Int. J. Agric. Biol. Eng. 15 (2022) 124–131. https://doi.org/10.25165/j.ijabe.20221501.6758.
47. K. Akarsu, G. Duman, A. Yilmazer, T. Keskin, N. Azbar, J. Yanik, Sustainable valorization of food wastes into solid fuel by hydrothermal carbonization, Bioresour. Technol. 292 (2019) 121959. https://doi.org/10.1016/j.biortech.2019.121959.
48. Z. Liu, A. Quek, S. Kent Hoekman, R. Balasubramanian, Production of solid biochar fuel from waste biomass by hydrothermal carbonization, Fuel. 103 (2013) 943–949. https://doi.org/10.1016/j.fuel.2012.07.069.
49. I. Pavkov, M. Radojčin, Z. Stamenković, S. Bikić, M. Tomić, M. Bukurov, B. Despotović, Hydrothermal Carbonization of Agricultural Biomass: Characterization of Hydrochar for Energy Production, Solid Fuel Chem. 56 (2022) 225–235. https://doi.org/10.3103/S0361521922030077.

50. K.G. Burra, M.S. Hussein, R.S. Amano, A.K. Gupta, Syngas evolutionary behavior during chicken manure pyrolysis and air gasification, Appl. Energy. 181 (2016) 408–415. https://doi.org/10.1016/j.apenergy.2016.08.095.
51. N.U. Saqib, M. Oh, W. Jo, S.K. Park, J.Y. Lee, Conversion of dry leaves into hydrochar through hydrothermal carbonization (HTC), J. Mater. Cycles Waste Manag. 19 (2017) 111–117. https://doi.org/10.1007/s10163-015-0371-1.
52. X. Chen, Q. Lin, R. He, X. Zhao, G. Li, Hydrochar production from watermelon peel by hydrothermal carbonization, Bioresour. Technol. 241 (2017) 236–243. https://doi.org/10.1016/j.biortech.2017.04.012.
53. S.K. Hoekman, A. Broch, C. Robbins, Hydrothermal carbonization (HTC) of lignocellulosic biomass, Energy and Fuels. 25 (2011) 1802–1810. https://doi.org/10.1021/ef101745n.
54. M. Wilk, M. Śliz, M. Gajek, The effects of hydrothermal carbonization operating parameters on high-value hydrochar derived from beet pulp, Renew. Energy. 177 (2021) 216–228. https://doi.org/10.1016/j.renene.2021.05.112.
55. A.J. Ashworth, J.P. Chastain, P.A. Moore, Nutrient Characteristics of Poultry Manure and Litter, Anim. Manure Prod. Charact. Environ. Concerns, Manag. (2020) 63–87. https://doi.org/10.2134/asaspecpub67.c5.
56. G.F. Antonious, E. Perkins, A.H. Cantor, Chicken manure increased concentration of organic sulfur compounds in field-grown onions, J. Environ. Sci. Heal. - Part B Pestic. Food Contam. Agric. Wastes. 44 (2009) 481–487. https://doi.org/10.1080/03601230902935303L.T. Contreras Montoya, S. Lain, M. Issa, A. Ilinca, 4 - Renewable energy systems, Hybrid Renew. Energy Syst. Microgrids. (2021) 103–177. https://doi.org/https://doi.org/10.1016/B978-0-12-821724-5.00013-1.
57. L.T. Contreras Montoya, S. Lain, M. Issa, A. Ilinca, 4 - Renewable energy systems, Hybrid Renew. Energy Syst. Microgrids. (2021) 103–177. https://doi.org/https://doi.org/10.1016/B978-0-12-821724-5.00013-1.
58. A. Demirbas, Higher heating values of lignin types from wood and non-wood lignocellulosic biomasses, Energy Sources, Part A Recover. Util. Environ. Eff. 39 (2017) 592–598. https://doi.org/10.1080/15567036.2016.1248798
59. K.C.R. Drudi, R. Drudi, G. Martins, G.C. Antonio, J.T.C. Leite, Statistical model for heating value of municipal solid waste in Brazil based on gravimetric composition, Waste Manag. 87 (2019) 782–790. https://doi.org/10.1016/j.wasman.2019.03.012.
60. J. Velebil, J. Malaták, J. Bradna, Mass yield of biochar from hydrothermal carbonization of sucrose, Res. Agric. Eng. 62 (2016) 179–184. https://doi.org/10.17221/73/2015-RAE.
61. I.C. Kantarli, A. Kabadayi, S. Ucar, J. Yanik, Conversion of poultry wastes into energy feedstocks, Waste Manag. 56 (2016) 530–539. https://doi.org/10.1016/j.wasman.2016.07.019.
62. H.S. Kambo, J. Minaret, A. Dutta, Process Water from the Hydrothermal Carbonization of Biomass: A Waste or a Valuable Product?, Waste and Biomass Valorization. 9 (2018) 1181–1189. https://doi.org/10.1007/s12649-017-9914-0.
63. M.Q. Orlando, V.M. Borja, Pretreatment of animal manure biomass to improve biogas production: A review, Energies. 13 (2020). https://doi.org/10.3390/en13143573.
64. E. Sermyagina, J. Saari, J. Kaikko, E. Vakkilainen, Hydrothermal carbonization of coniferous biomass: Effect of process parameters on mass and energy yields, J. Anal. Appl. Pyrolysis. 113 (2015) 551–556. https://doi.org/10.1016/j.jaap.2015.03.012.
65. M. Van Peer, L. Frooninckx, C. Coudron, S. Berrens, C. Álvarez, D. Deruytter, G. Verheyen, S. Van Miert, Valorisation potential of using organic side streams as feed for tenebrio molitor, acheta domesticus and locusta migratoria, Insects. 12 (2021) 1–32. https://doi.org/10.3390/insects12090796.